Aus der Klinik für Neurochirurgie
der Heinrich-Heine-Universität Düsseldorf
Direktor: Univ.-Prof. Dr. med. Hans-Jakob Steiger

Anatomic variations of the distal basilar artery and basilar tip aneurysms: Epidemiologic and morphologic correlations

Dissertation

zur Erlangung des Grades eines Doktors der Medizin
der Medizinischen Fakultät der Heinrich-Heine-Universität Düsseldorf

vorgelegt von
Dott. Angelo Tortora
2018

Als Inauguraldissertation gedruckt mit Genehmigung der Medizinischen Fakultät der

Heinrich-Heine-Universität Düsseldorf

gez.:

Dekan: Univ.-Prof. Prof. Dr. Nikolaj Klöcker

Erstgutachter: PD Dr. K. Beseoglu
Korreferent: Prof. Dr. B. Turowski

Zusammenfassung

Einleitung: Anatomische Variationen der posterioren, zerebralen Zirkulation sind häufige Befunde bei der invasiven und nicht-invasiven Diagnostik der intrakraniellen Gefäße. Die anatomischen Variationen der distalen Basilararterie entstehen während der Ontogenese dieses Gefäßes, die von der dorsalen Teilung der primitiven Carotisarterie herrührt. Eine Unterbrechung während dieser Entwicklung führt zur Persistenz der unreifen Form. "Unreife" Variationen werden als gutartige Befunde ohne pathologischen Wert definiert, welche lediglich bei begleitenden neurovaskulärer Erkrankungen behandlungsbedürftig werden aufgrund des Einflusses auf die Blutversorgung. Über diesen hämodynamischen Einfluss und ihre Rolle bei der Pathogenese intrakranieller Aneurysmen ist wenig bekannt. Das Ziel dieser Studie war es, zu untersuchen, ob anatomische Variationen der distalen Basilararterie mit der Bildung von Aneurysmen an dieser Stelle zusammenhängen und zu deren Ruptur beitragen.

Methoden: In einer retrospektiven Studie wurden Patienten mit distalen Basilarisaneurysmen untersucht, die zwischen Januar 2000 und Februar 2017 in der neurochirurgischen Klinik der Heinrich-Heine-Universität Düsseldorf behandelt wurden. Die Aneurysmen des Basilariskopfes, des präkommunizierenden Segments der hinteren zerebralen Arterie (P1) und der vordere pontomesencephale Abschnitt der Arteria cerebelli superior (s1), die alle einen gemeinsamen embryologischen Ursprung haben, wurden für die Studie berücksichtigt.

Mit Hilfe invasiver und nichtinvasiver Bildgebungen konnte das Vorliegen einer unvollständigen Fusion der distalen Basilararterie, einer fötalen posterioren kommunizierenden Arterie und einer unreifen P1-P2A-Verbindung festgestellt werden. Die Prävalenz dieser embryologischen Muster in der oben genannten Population wurde mit einer Kontrollgruppe von Patienten mit Aneurysmen in anderen Teilen des intrakraniellen Kreislaufs verglichen.

Ergebnisse und Diskussion: Ein unreifer P1-P2A-Übergang wurde bei allen 5 Patienten mit P1-Aneurysma festgestellt. Es zeigt sich eine statistisch relevante Korrelation zwischen unreifer Verbindungsmorphologie und dem Vorhandensein eines

P1-Aneurysmas (P = 0,015). Der Grund für diese Beziehung ist unbekannt und kann nicht aus den hämodynamischen Theorien der Aneurysmenbildung abgeleitet werden.

Es wurde eine positive Korrelation zwischen dem Vorhandensein von Basilariskopf- oder S1-Aneurysmen und einem unreifen P1-P2A-Übergang festgestellt. Zudem war ein unreifes Fusionsmuster der distalen Basilararterie in allen drei Untergruppen von Aneurysmen häufiger als in der Kontrollpopulation. Aufgrund der begrenzten Stichprobengröße erreichten diese Ergebnisse keine statistische Signifikanz. Es ergab sich keine Korrelation zwischen dem Vorhandensein einer fetalen posterioren Kommunikationsarterie und dem Vorhandensein eines Aneurysmas in der distalen Basilararterie.

Schlussfolgerungen: Das Vorhandensein eines unreifen P1-P2A-Übergangs sollte als Risikofaktor für Aneurysmen des P1-Segments der PCA angesehen werden. Gründe für diese Korrelation sind noch unbekannt und können in der Struktur der Wand dieses embryologischen unreifen arteriellen Segments liegen. Multizentrische Studien mit einer größeren Patientenprobe sind erforderlich, um die Rolle eines unreifen P1-P2A-Übergangs in der Pathogenese von S1- und basilaren Spitzenaneurysmen sowie den Einfluss von unreifen Fusionsmustern der distalen Basilararterie auf die Pathogenese aller drei zu bestätigen.

Abstract

Presentation and goals of the study: Anatomical variations are common findings during invasive and non-invasive diagnostic of posterior cerebral arterial circulation. These alterations of the traditional "textbook" anatomy are a manifestation of the wonderful mechanism behind the evolution of the cerebral vascular three, which can be appreciated in the studies of comparative anatomy and has the human intracranial arterial system as the most elaborate and marvelous result. The anatomical variations of the distal basilar artery originate during the ontogenesis of this vessel that derives from the dorsal division of the primitive carotid artery. A stop during the maturation process results in the persistence on an immature form.

"Immature" variations are commonly interpreted as benign conditions without pathological significance and presenting only some implications during the treatment of concomitant neurovascular conditions due to the alteration of blood supply related to their presence. Little is known about their hemodynamic impact and their role in the pathogenesis of intracranial aneurysms.

The goal of this study was to investigate if anatomical variations of the distal basilar artery are related to the formation of aneurysms in this location and contribute to their rupture.

Methods: In a retrospective study we analyzed patients with distal basilar artery aneurysms who were treated in the Neurosurgical Department of the Heinrich Heine University, Düsseldorf between January 2000 and February 2017. The aneurysms of the basilar tip, of the precommunicating segment of the posterior cerebral artery (P1) and of the anterior pontomesencephalic segment of the superior cerebellar artery (s1), that share common embryological origin, were considered for the study.

The presence of an incomplete fusion of the distal basilar artery, of a fetal posterior communicating artery and of an immature P1-P2A junction was identified on invasive and non-invasive imaging records of the patients. The prevalence of these embryological patterns in the above mentioned population was compared to a control group of patients with aneurysms in other portions of the intracranial circulation.

Results and discussion: An immature P1-P2A junction was encountered in all 5 patients with P1 aneurysm, resulting in a statistically relevant correlation between immature junction morphology and presence of P1 aneurysm (P= 0.015). The reason for this relation is unknown and can´t be deduced from the hemodynamic theories of aneurysms formation, creating the immature P1-P2A junction an increased blood flow turbulence distal to the location of the P1 aneurysms.

A positive correlation was encountered between the presence of basilar tip or S1 aneurysms and an immature P1-P2A junction.

An immature fusion pattern of the distal basilar artery was also more common in all three subgroups of aneurysms compared to the control population. Probably due to the limited sample size these results didn´t reach statistical significance.

A correlation between the presence of a fetal posterior communicating artery and the presence of an aneurysm in the distal basilar artery could be excluded.

Conclusions: The presence of an immature P1-P2A junction should be considered as a risk factor for aneurysms of the P1 segment of the PCA. Reasons for this correlation are yet unknown and may lie in the structure of the wall of this embryological immature arterial segment.

Multicenter trials are required to collect a bigger patient´s sample to confirm the role of an immature P1-P2A junction in the pathogenesis of s1 and basilar tip aneurysms and the impact of immature fusion patterns of the distal basilar artery in the pathogenesis of all three aneurysm locations considered in this study.

Abbreviations

Arteries

ACA	anterior cerebral artery
AChA	anterior choroidal artery
ACoA	anterior communicating artery
AICA	anterior inferior cerebellar artery
AntSpA	anterior spinal artery
AntThaP	anterior thalamoperforators
BA	basilar artery
lPChA	lateral posterior choroidal artery
MCA	middle cerebral artery
mPChA	medial posterior choroidal artery
PCA	posterior cerebral artery
PComA	posterior communicating artery
PedP	peduncular perforators
PICA	posterior inferior cerebellar artery
PosThaP	posterior thalamoperforators
SCA	superior cerebellar artery
VA	vertebral artery
VBJ	vertebrobasilar junction

PCA

P1	precommunicating segment
P2	postcommunicating segment
P2A	crural segment
P2P	ambient segment
P3	quadrigeminal segment
P4	calcarine Segment

SCA

s1	anterior pontomesencephalic segment
s2	lateral pontomesencephalic segment
s3	cerebellomesencephalic segment
s4	cortical segment

AICA

a1	anterior pontine segment
a2	lateral pontine segment
a3	flocculonodular segment
a4	cortical segment

Others

3DRA	3D rotational angiography
AR	aspect ratio (dome height/ neck width)

CT	computed tomography
CTA	computed tomography angiography
DSA	digital subtraction angiography
DNR	dome to neck ratio (dome width/ neck width)
MRT	magnetic resonance imaging
MRA	magnetic resonance angiography
SAH	subarachnoid hemorrhage

Summary

1 Introduction ..... - 1 -
1.1 Embryology of the distal basilar artery ..... - 1 -
1.2 Anatomy of the distal basilar artery ..... - 3 -
1.3 Anatomical variations of the distal basilar artery ..... - 5 -
1.4 Distal basilar artery aneurysms ..... - 10 -
1.5 Management of distal basilar artery aneurysms ..... - 12 -
2. Background and Goals of the Study ..... - 16 -
3 Materials und Methods ..... - 18 -
3.1 Data ..... - 18 -
3.2 Inclusion and exclusion criteria ..... - 18 -
3.3 Parameters analyzed ..... - 18 -
3.4 Interpretation of imaging diagnostics ..... - 20 -
3.5 Statistical analysis ..... - 20 -
3.5.1 Chi-squared test ..... - 20 -
3.5.2 Fisher's exact test ..... - 21 -
3.5.3 Independent samples t-test ..... - 21 -
4 Results ..... - 22 -
4.1 Patient demographics ..... - 22 -
4.2 Aneurysm location ..... - 22 -
4.3 Aneurysm presentation ..... - 22 -
4.4 Aneurysm treatment ..... - 23 -
4.5 Aneurysm morphology ..... - 23 -
4.6 Distal basilar artery anatomy ..... - 25 -
5 Discussion ..... - 33 -
5.1 Study population; demography, location, presentation and treatment of the aneurysms of distal basilar artery. ..... - 33 -
5.2 Aneurysm morphology ..... - 35 -
5.3 Correlation between aneurysms and anatomical variations ..... - 36 -
5.4 Aneurysms and distal basilar artery fusion pattern ..... - 37 -
5.5 Aneurysms and morphology of P1-P2 junction ..... - 39 -
6 Conclusions: ..... - 41 -
References ..... - 42 -

1 Introduction

1.1 Embryology of the distal basilar artery

At the end of the 3 rd week of the embryonic development the amniotic fluid provides directly for the nutrition of the primitive nervous system and metabolites diffuse through the ependyma covering the neural crest (1, 3).

As the neural crest folds longitudinally by the fourth week of pregnancy forming the neural tube, a connective tissue will form the meninx primitiva that envelops the neural tube (3, 6). Endothelial cells in the meninx primitiva proliferate and organize to constitute a superficial plexus without venous of arterial differentiation (2).

Two dorsal aortas and the cardinal veins join the developing cerebral vascularization leading to the differentiation of the meningeal plexus in arteries, veins on the surface of this primitive meninx and capillaries (3).

At the 24th day the precursor of posterior circulation is constituted by a plexus of vessels along the ventral surface of the rhombencephalon (3, 6). They will coalesce to form the bilateral longitudinal neural arteries, the precursor of the basilar artery (4, 5).

After the formation of 6 pairs of aortic arches a branch extends from the first arch forming the trigeminal artery that anastomoses with the longitudinal neural arteries providing the first supply for the primitive posterior circulation (3). The trigeminal artery will later be included in the carotid system and together with three other branches of the carotid artery (hypoglossal, otic and proatlantal artery) supply between the 24th and 29th day the posterior circulation (3).

At this stage, the paired precursors of the carotid arteries end ventral to the prosencephalic vesicle (3, 6). Around day 29th, this vessel splits in a posterior and in a ventral branch which will divide again to form an arterial ring around the neck of each telencephalic vesicle which later forms the anterior cerebral artery (anterior portion of the ring) and the anterior choroidal artery (posterior portion of the ring), (6).

Lateral branches of the anterior choroidal artery (AchA) will form its telencephalic territory which in the adult configuration will correspond to the cortical posterior cerebral artery (PCA) territory (3).

The posterior division of the internal carotid artery (ICA) reaches the cephalic end of the ipsilateral ventral longitudinal artery to form the posterior communicating artery (PComA). This artery will originate the precommunicating segment (P1) of the PCA and the distal part of the basilar artery (6).

The development of the PComA leads to regression of the transient hypoglossal, proatlantal, otic and trigeminal anastomoses between day 29 and 32 (3). After regression of the trigeminal artery, the flow direction in the basilar artery inverts becoming centrifugal as the vertebral artery doesn´t exist at this stage (3).

The further development of mesencephalon and rhombencephalon with appearance of tectum and primitive cerebellum stimulates the growth of new branches of the caudal division of the internal carotid system. These are the diencephalic, the mesencephalic and superior cerebellar artery (6).

As the volume of the primordial brain increases, the need for oxygen and metabolites leads to the development of invaginations of the meninx primitiva in the ventricular lumen which forms the choroid plexi at the end of the 6th week (1, 3).

From the posterior division of the ICA originates the posterior choroidal artery to feed the choroid plexus of the 3rd ventricle (3, 6). The plexus in the 4th ventricle is vascularized by a vessel from the basilar artery/longitudinal neural artery which will later evolve to form the posterior inferior cerebellar artery (3, 6).

Between the 6th and 7th embryonic week, the longitudinal arteries fuse in the midline caudo-cranially to form the basilar artery (3, 7).

The longitudinal anastomoses between the segmental cervical arteries from the subclavian artery to the craniocervical junction will than form the vertebral artery (6, 8).

The development of the vertebral artery and the resulting craniopetal flow in the basilar artery facilitates further development and annexation of the diencephalic-mesencephalic trunk of the ICA caudal division (3). Selected cortical territories of the anterior ICA division will be annexed by telencephalic branches of the posterior choroidal artery and later by the diencephalic artery forming the PCA (6).

The primitive territory of the carotid system extends caudally in the posterior fossa to the level of the transient trigeminal artery.

1.2 Anatomy of the distal basilar artery

This chapter summarizes the anatomy of the distal basilar artery considering the course of the artery distal to the anterior inferior cerebellar artery (AICA) origin, the proximal part of its main branches (anterior pontine segment or s1, P1, crural segment or P2A) and relevant smaller arteries and perforators branching from above mentioned vessels. For embryological reasons, that link the PComA to the distal basilar artery its course and branches will also be described here.

The basilar artery distal to its origin at the pontomedullary junction courses upward in the prepontine cistern encased dorsally by the basilar sulcus in the midline of the pons (9). Distal to the AICA origin the basilar artery gives rise to 1-10 middle and rostral perforators, respectively (9, 10). Middle perforators are located between AICA and the posterolateral arteries, one of the pontine arteries. They branch from the posterolateral surface of the basilar artery running in the basilar sulcus and enter the pons on its edge to feed its medial portion (9, 10). On the last centimeter of the basilar artery the rostral basilar perforators originate. Their vascular territory overlaps with the posterior thalamo-perforating arteries (9, 10).

Following the basilar artery distally the superior cerebellar artery (SCA) is encountered which branches between PCA´s P1 segment and 7 mm below PCA´s origin directly from the basilar artery (average 2.5 mm), (11). The first Segment of the SCA is called s1 and originates underneath the oculomotor nerve, courses lateral around the mesencephalon and ends on the anterolateral brainstem where the artery crosses the tentorial incisura (9).

The SCA usually duplicates in a rostral and a caudal branch somewhere on its course between its origin and the S3 segment (9).

The average diameter of the basilar artery at the level of the SCA´s origin is 3.5 mm and approximately 4.1 mm at the level of the basilar bifurcation (11).

The basilar artery terminates usually with paired posterior cerebral arteries in the interpeduncular cistern which extends supra- and infratentorial at the level of the anterior tentorial incisura (11). The interpeduncular cistern is bordered by cerebral peduncles posteriorly and Liliequist´s membrane ventrally, laterally and caudally. The roof of the interpeduncular cistern is formed by the posterior perforated substance (12).

The basilar bifurcation is usually located in the interpeduncular fossa but can be encountered somewhere between the ponto-mesencephalic junction and the level of the mammillary bodies on the floor of the third ventricle. The ventricle floor can be cranially dislocated with high riding basilar tips. The distance between the basilar tip and the mammillary bodies is in average 8.1 mm (range 0-14mm), (11, 13).

Considering the biclinoidal line that connects the anterior and posterior clinoidal process, the basilar apex is above the dorsum sellae in 70% of the patients, at level with the dorsum sellae in 20% and below in 10% (11, 13).

The P1 segment represents the first segment of the PCA and extends from the basilar bifurcation to the point where PComA joins PCA. It courses laterally parallel to the s1 segment and cranial to the oculomotor nerve. The length of the P1 segment varies between 3 and 14 mm (9).

Posterior thalamo-perforating arteries originate from the superior and posterior surface of the middle third of P1. They run superiorly and posteriorly to the posterior perforated substance, cerebral peduncle and mammillary bodies. There are on average 4 but can be up to 12 with bilateral origin or unilateral origin and bilateral distribution. The regions supplied by these perforators comprise the anterior portion and part of the posterior portion of the thalamus and hypothalamus, the subthalamus and the posterior limb of the internal capsule (9, 14).

The second segment of the PCA is called P2A and runs in the crural cistern between cerebral peduncle and uncus under the optic tract and basal vein of Rosenthal.

Relevant branches of the proximal PCA segments are constituted by the circumflex arteries, originating from P1-P2A to feed the cerebral peduncles, tegmentum, medial geniculate body, tectum and pulvinar, the peduncular perforating arteries from P2A that feed the cerebral peduncles and the thalamogeniculate arteries originating from the P2A-P2P (ambient segment) junction to feed the area of the geniculate bodies (9, 13).

The medial posterior choroidal artery (MPChA) usually branches from the P1 segment as a single vessel or as multiple arteries coursing in the crural, ambient and quadrigeminal cistern to reach the velum interpositum on the roof of 3rd ventricle. This artery supplies the cerebral peduncle, tegmentum, geniculate bodies, colliculi, pulvinar, pineal gland and medial thalamus (9, 13).

The PcomA originates from the posteromedial portion of the internal carotid artery midway between the origin of the ophthalmic artery and the carotid bifurcation. It courses in a medial and dorsal direction above the sella turcica, below the tuber cinereum, above and medial to the oculomotor nerve to join the PCA at the P1-P2 junction. Together with the proximal basilar bifurcation it forms the posterior portion of the circle of Willis (9, 13).

On average eight (4-14) anterior thalamo-perforating arteries arise from the superior and lateral portion of the PComA. Their origin is distributed along the whole vessel although the anterior half has a bigger density of vessels. Anterior thalamoperforators course superiorly to reach the floor of the 3rd ventricle and supply the posterior hypothalamus, optic chiasm, anterior thalamus, posterior limb of the internal capsule and subthalamus (9, 13).

1.3 Anatomical variations of the distal basilar artery

Incomplete fusion process of the ventral longitudinal arteries may give origin to fenestrations of the basilar artery with an incidence of 2.1% according to Rhoton (see Figure 1.3.1). In 94% of cases, this anomaly involves the proximal basilar artery. AICA or perforating branches may originate from the fenestrated segment (9).

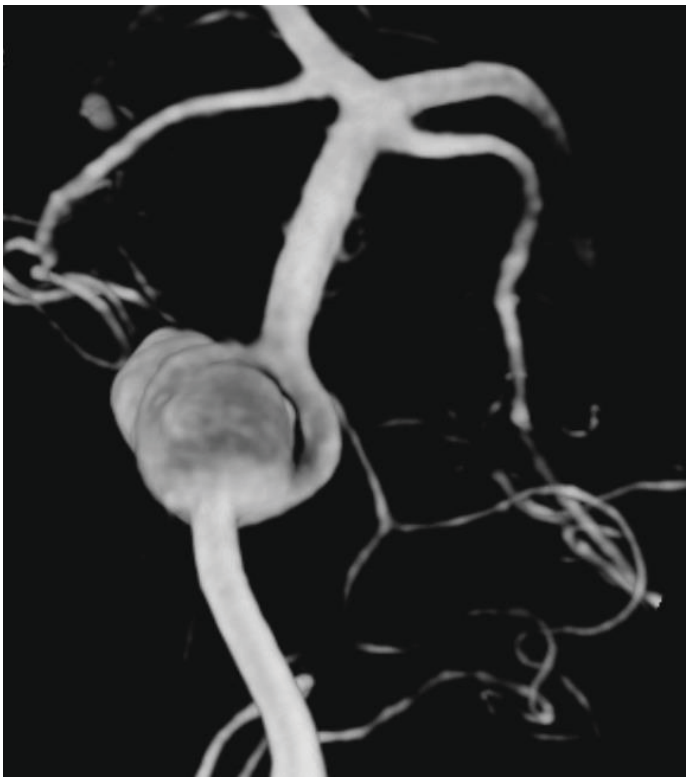

Figure 1.3.1: The 3D rotational angiography (3DRA) shows a fenestration in the proximal basilar artery associated with a ruptured fusiform aneurysm.

The trigger for the maturation of the primitive posterior circulation is the regression of the trigeminal artery. The resulting caudocranially directed fusion process of the basilar artery bears a range of morphological-hemodynamic variations. The later the transient trigeminal artery regresses, the less hemodynamic importance to supply the PCA, the vertebro-basilar system will have and the more caudal the process of fusion will stop (3). In this setting the ICA´s contribution to the supply of the PCA territory remains dominant and the SCA will originate from P1. This condition can be encountered mono- or bilaterally.

According to Lasjaunias (3) three types of anatomical configurations of the basilar tip have been described based on the SCA´s origin (Figure 1.3.2). If the cerebellar artery originates bilaterally from P1 the disposition will be called *symmetrical caudal fusion*. *Cranial symmetrical fusion* describes a disposition where the SCA originates directly from the basilar trunk bilaterally. In the pattern called *asymmetrical caudal fusion,* one side presents a s1 originating from P1 and the other side a cerebellar artery branching from the basilar tip.

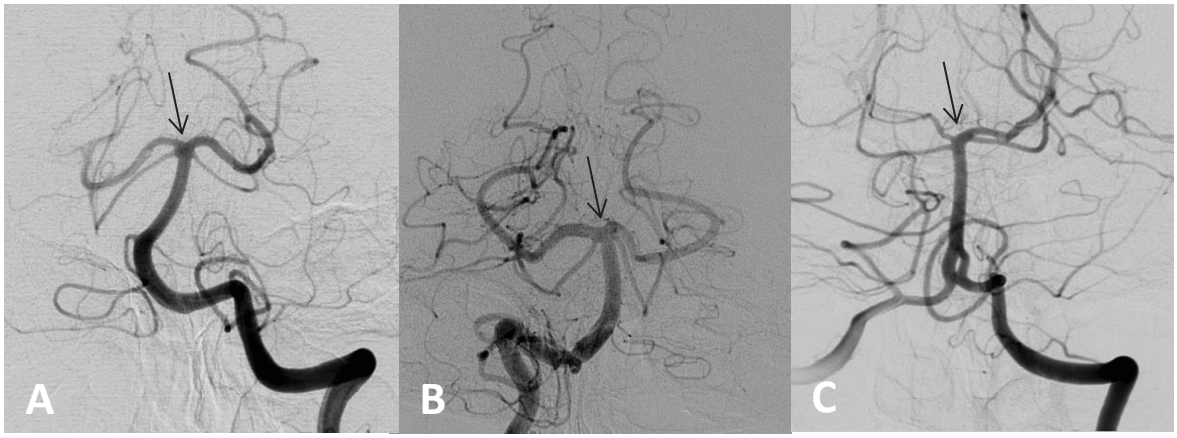

Figure 1.3.2 Symmetrical cranial fusion of this basilar tip. Both s1 originate directly from the basilar trunk (A). Panel B shows a symmetrical caudal fusion. s1 originate directly from P1 bilaterally. The angiogram in panel C shows an asymmetric configuration where the right s1 originates from the basilar artery whereas the left s1 branches from P1. The arrows in the figures A-C indicate the basilar bifurcation.

The pattern presenting a duplicated origin of s1 from both P1 and s1 is considered caudally fused when bilaterally existent or asymmetric caudal fusion when it is unilateral (Figure 1.3.3).

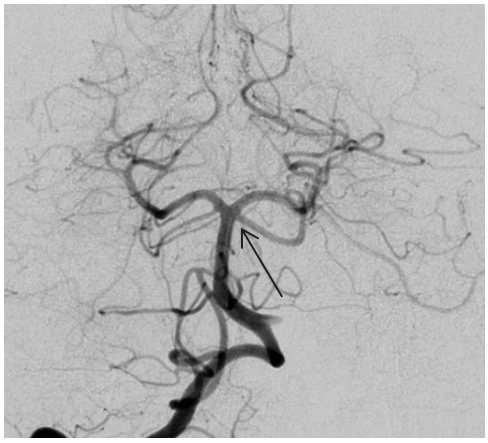

Figure 1.3.3: The figure shows an *asymmetric caudal fusion* where the left s1 originates from the basilar artery whereas the right s1 has a duplicated origin from both P1 and basilar artery. The arrow indicates the basilar bifurcation.

In a series of 47 patients undergoing cerebral angiography Campos et al. (15) encountered cranial symmetrical fusion in 30.4% of the population, caudal symmetrical fusion in 26.1% and caudal asymmetrical configuration in the remaining 43.5%.

In case of symmetrical cranial or caudal fusion, posterior thalamoperforators from the basilar tip will supply each side and form anastomoses in the interpeduncular fossa in 60-80% of patients. In patients with asymmetric fusion, a common trunk originating usually from the most cranial P1 segment will supply both sides (3).

In an anatomical study, half of the specimens showed a normal configuration of the posterolateral portion of the circle of Willis with P1s being more prominent than PComAs (6, 24). The other half presented some variations like fetal PComA configuration, with PComA being thicker than P1 and providing the major supply to the P2 segment (unilaterally in 20% and bilaterally in 2%) or on the other side a hyper mature configuration with hypoplastic PcomA (26% unilaterally or 6% bilaterally). In 18% of the specimens a hypoplastic PcomA with a contralateral fetal configuration was seen. Absence of both PcomAs and P1s with ACh supplying the PCA territory is very

uncommon (16). Hypoplastic PComAs and P1s usually originate a normal number of regularly sized perforators (Figure 1.3.4).

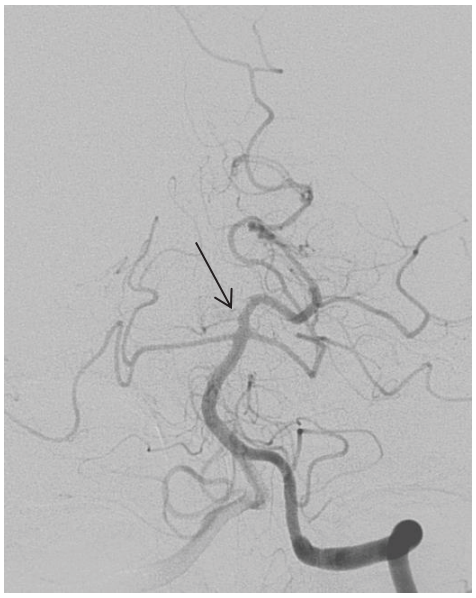

Figure 1.3.4: The aplasia of right P1 is shown. There is no contribution of posterior circulation to the right PCA territory (arrow). On the right side the P1 is represented by posterior thalamoperforators and a peduncular artery.

Van Raamt et al. (17) named the pattern with PcomA being more prominent than P1 *partial fetal configuration*. The absence of P1 was called "*full fetal configuration"*.

In case of fetal configuration of the PcomA, P1 has a mean length of 9 mm compared to 7 mm in case of a normal morphology (9).

Reversal of flow in the distal basilar artery after development of the vertebral arteries from cervical segmental arteries also produces geometrical variations at the PcomA-PCA junction. In a fetal PcomA configuration, the Pcom-P2A angle is around 180°, being P2 of the natural continuation of PcomA and the P1-P2 angle is around 90°. During the development, as P1 acquires the dominant role in the supply of the P2A segment, P1-P2 angle increases and the junction turns into a curve. Many variations between these two antipodes are routinely encountered (Figure 1.3.5).

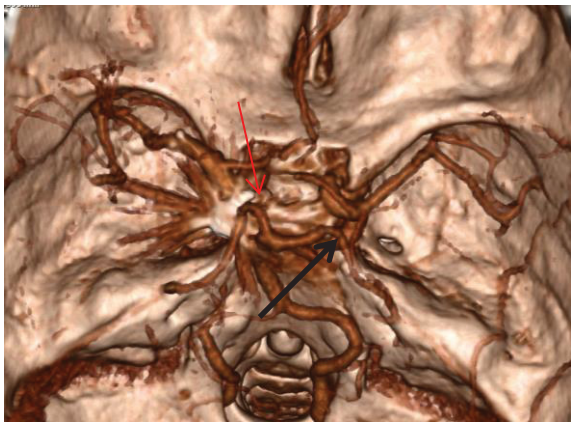

Figure 1.3.5 CTA showing a fetal P1-P2A junction on the left side with a sharp angle between the two vessels (red arrow). Note the absence of a fetal PComA that would explain this conformation. On the right side the P1-P2A junction can be assimilated to a curved line.

Rare variations are represented by:

- hypercranial fusion pattern with fusion of PcomAs and origin of s1s, P1s from the fused PcomAs,
- fenestrations or duplications of P1, P2, SCA, PcomA,
- persistence of trigeminal artery,
- origin of SCA, AICA or PICA directly from ICA representing a partial persistence of trigeminal artery filling the territories of ventral longitudinal arteries (3).

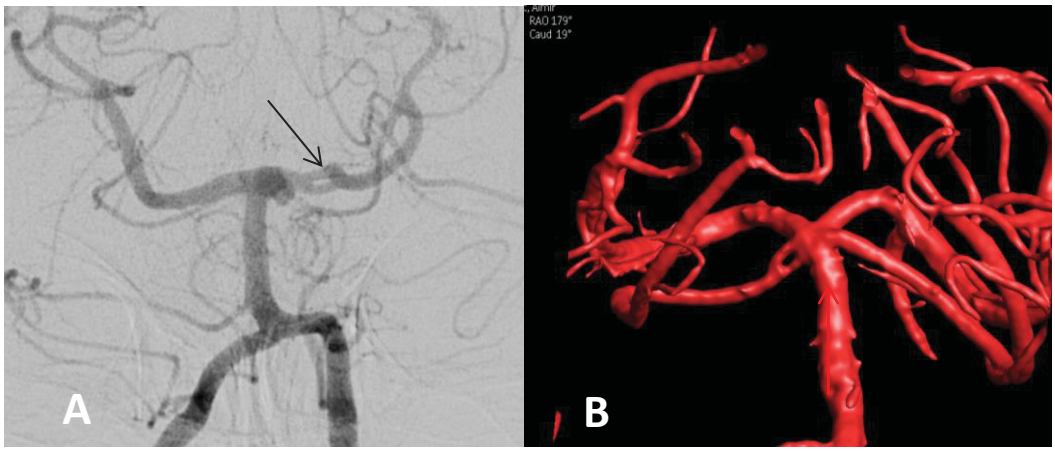

Figure 1.3.5: Panel A shows a fenestration of the left-sided distal P1 segment in a patient with a dorsally projecting basilar tip aneurysm. The 3DRA demonstrates a fenestration at the origin of the right SCA (B).

A duplicated origin of the SCA is commonly encountered (Figure 1.3.6), however a triplicated SCA is a rare variation (3, 9).

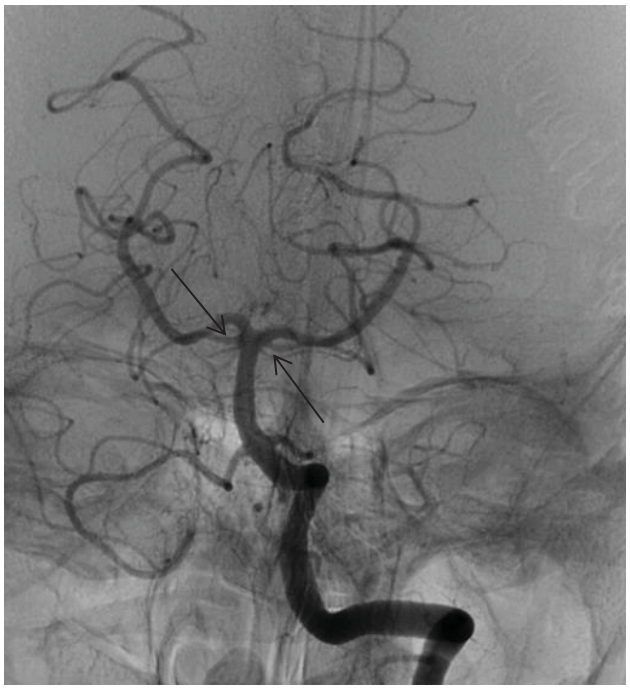

Figure 1.3.6: The angiography shows a bilateral duplicated origin of the SCA (arrows).

Persistence of a trigeminal, otic, or hypoglossal artery in adult life with resulting vertebral or basilar hypoplasia/aplasia are typically reported unilaterally and usually found incidentally, however they may be responsible for ischemic events or aneurysms (3, 9).

1.4 Distal basilar artery aneurysms

Aneurysms of the posterior cerebral circulation represent 10 to 18% of all intracranial aneurysms (18). The most common location is the basilar tip corresponding to 49-72% of cases while PCA and SCA aneurysms are comparably rare (19-26). The average age at diagnose is 50.3 to 53.9 years and female prevalence with 72% is seen (19-26).

Distal basilar artery aneurysms share the same risk factors for development and rupture with other cerebral aneurysms including patient age, previous aneurysmal rupture and modifiable socio-dietetic factors like tobacco smoking, excessive alcohol intake and arterial hypertension (27, 28).

Genetic predisposition such as female sex, familial cumulation and various syndromic diseases like autosomal-dominant polycystic kidney disease and Ehlers-Danlos syndrome type IV are also well known. In recent years, several genetic loci have been proposed to be associated with familial linkage (27, 28).

The formation and evolution of an aneurysm is believed to be a multifactorial process where environmental and genetic risk factors interact with hemodynamic loads, wall biomechanics, mechanobiology, and peri-aneurysmal environment of the affected artery (64).

Saccular aneurysms being the most common aneurysm type in the basilar tip, P1 and s1 locations develop according to hemodynamic theories in regions of increased hemodynamic stress such as bifurcations and on the convex side of a curvature of a vessel (9). Increased hemodynamic loads might trigger focal degenerative mechanisms at the vessel wall, that are supposed to be associated to abnormal NO production in response to high shear stress and to inflammation from thrombus formation in regions of low shear stress (62).

It has been suggested that some aneurysms rupture and bleed shortly after formation and thus are rarely detected as incidental findings and that aneurysms without early rupture remain stable through some healing process (63). Aneurysm rupture is thus the ultimate consequence of the walls failure to contain the hemodynamic loads and rupture occurs when wall stress exceeds wall strength. However, the detailed mechanisms that weaken the wall and drive the evolution of the aneurysm towards stabilization or rupture are not fully understood (62).

Aneurysms of the posterior cerebral circulation harbor a 2.5 fold increased relative risk for rupture as compared to equivalent lesions in the anterior circulation (29). Additionally, when ruptured they lead to worse clinical condition at admission, greater in-hospital mortality and lower overall-survival as compared to lesions of the anterior circulation (30, 31). Patients with ruptured aneurysms of the anterior circulation present a 77% survival-rate after two days compared to a 32% survival-rate for posterior circulation aneurysm patients (30, 31). The 30 day survival is 57% vs. 11%, respectively (30, 31). Deep location in proximity of the brainstem, higher occurrence of intraventricular hemorrhage and hydrocephalus may partially explain the worse outcome.

Other symptoms associated with distal basilar artery aneurysms are related to thromboembolic manifestations, symptoms of brainstem compression like gait and balance instability or weakness due to compression of the cerebral peduncle if the aneurysm reaches a critical size. Further non hemorrhagic manifestations include cranial nerve deficits like oculomotor, trochlear or abducens nerve palsy, trigeminal affection or obstructive hydrocephalus (32, 33).

1.5 Management of distal basilar artery aneurysms

Distal basilar artery aneurysms are complex lesions for both endovascular treatment and microsurgery due to their deep location, intimal relation with the brainstem and an intricate network of highly eloquent perforating vessels. The therapy has to be individualized for each patient according to rupture status, neurological condition at admission, morphology of the aneurysm, patient age and presence of comorbidities.

Ruptured aneurysms are primarily treated to avoid rerupture with the exception of patients where severe hemodynamic compromission or poor medical-neurological prognosis represents a contraindication. Indication for treatment of unruptured lesions is based on the morphology of the aneurysm, age, medical condition of the patients and presence of modifiable risk factors for rupture in the anamneses (18).

The advent and widespread use of endovascular techniques and results of the International Subarachnoid Aneurysm Trial (ISAT) switched the treatment paradigm for lesions located in the posterior circulation from microsurgery to endovascular therapy (34).

Nowadays, coil embolization represents the first therapeutic choice (18). The procedure offers protection from rerupture, is time effective and does not require antiplatelet therapy. However, coil embolization may be limited by aneurysm morphology, e. g, in aneurysms with wide neck a complete occlusion can only be achieved in 15% vs 85% of lesions with narrow neck (35). In this situation, coil procedure can be assisted with a balloon catheter which is temporary inflated at the level of the aneurysm neck to avoid coil herniation into the parent artery during the coiling process. This also allows for a higher coil density in the aneurysm (36). Potential risks associated with this procedure

are thromboembolic events, risk of arterial injury during inflation of the balloon and aneurysm rupture.

Broad neck aneurysms can also be treated with stent assisted coiling (18, 37, 38). The microcatheter for coil application can deliver the coils trough the stent meshes or alternatively after intraaneurysmal positioning of the microcatheter for coiling a second catheter delivering the stent is introduced avoiding the coil application through the meshes of the stent.

For broad neck basilar tip aneurysms a so called “Y stent” technique can be used to protect both PCAs before coiling (37, 38). The first stent is usually an open cell device and is positioned in the PCA that is more difficult to reach. The second stent is positioned in the second PCA and the coils can then be safely deployed into the aneurysm. However, the patient needs to be loaded with dual antiplatelet therapy periinterventionally increasing the hemorrhagic risk in patients with ruptured aneurysms. Additionally, stent use increases the risk of perforator occlusion or late development of intraluminal stenosis.

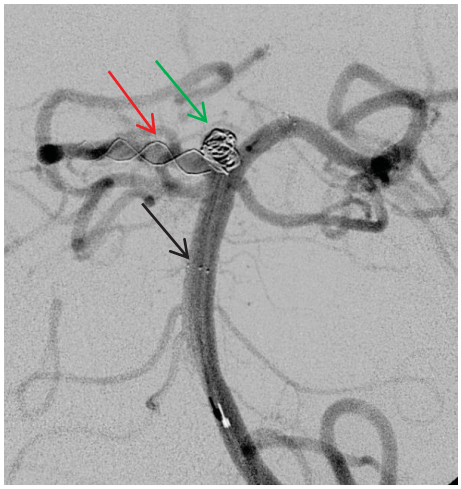

Figure 1.5.1: The angiography shows a basilar tip aneurysm treated with “Y stent” technique. The first stent (black arrow) was implanted from the basilar artery to the left P1. The second device (red arrow) was used to protect the right P1. The aneurysm (green arrow) could then be successfully coiled.

Use of liquid high viscosity polymers (e.g. Onyx 500) for aneurysm embolization is described with aneurysms presenting a complex geometry or that recur after coiling (39). The main limitations of polymer embolization are the need for antiplatelet therapy,

the necessity of balloon protection of the parent artery during injection and no available long term outcome data.

Reduction of blood flow near the aneurysm neck with flow diverting stent systems while preserving flow into parent vessel and neighboring branches provides delayed thrombosis of the aneurysm, followed by shrinkage of the aneurysm sac as the thrombus organizes and retracts. Thus, flow diversion treats the diseased segment harboring the aneurysm instead of treating the aneurysm itself.

In the posterior circulation flow diverters are mostly indicated for fusiform basilar aneurysms (40, 41). Their use harbor a risk for incomplete aneurysmal occlusion, ischemic stroke, delayed intracerebral hemorrhage and subarachnoid hemorrhage and perforator occlusion. Need for antiplatelet therapy and delayed occlusion of the aneurysm further limit their use in subarachnoid hemorrhage (SAH).

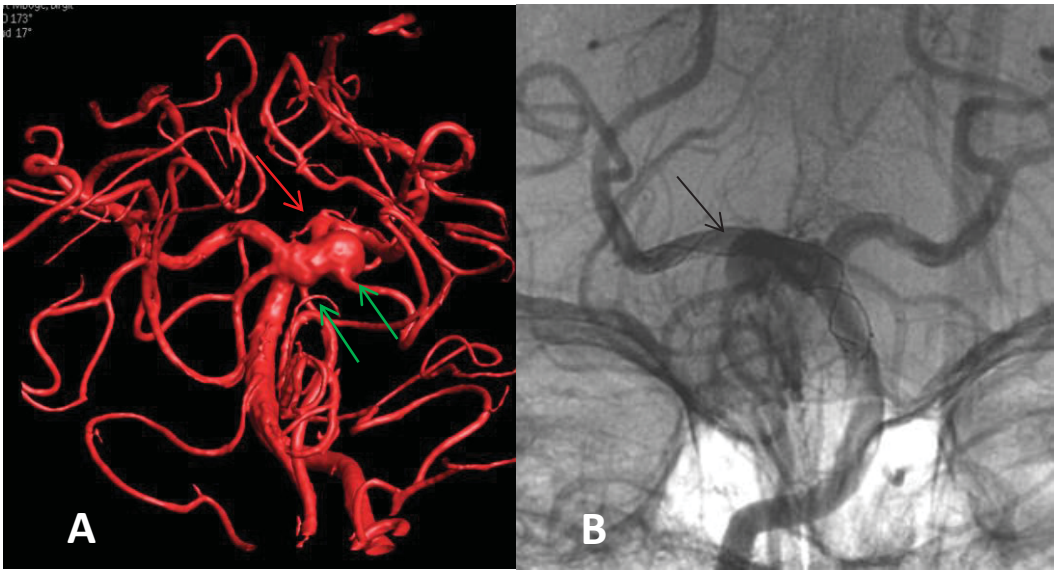

Figure 1.5.2: Panel A shows a complex dysplastic aneurysm involving the origin of the right P1 (red arrow) and of a duplicated SCA ipsilateral (green arrows). The aneurysm was treated with a flow diverter, which is evidenced by the black arrow (B).

In the setting of SAH coil embolization is preferred over stent or flow diverter application, when possible, facilitating a fast and safe aneurysm occlusion and minimizing the risk of rerupture. A staged therapy to provide a durable occlusion of the aneurysm is more desirable than a high risk therapy in the acute phase with higher complication rate (18).

At present, surgery for basilar tip aneurysms should be reserved to high volume neurovascular centers to treat patients not suited for endovascular therapy (18). Surgical treatment of basilar tip aneurysm can be performed with subtemporal, pterional or transcavernous approach (18). Selection of the appropriate approach is based on surgeon´s experience, position of the basilar bifurcation compared to the posterior clinoidal process and the projection of aneurysm. Anterior and superior projecting aneurysms are comparably more comfortable to treat surgically, while posterior projecting lesions are the most complex to treat (42).

2. Background and Goals of the Study

With an increasing number of incidentally diagnosed asymptomatic aneurysms due to a more widespread use of non-invasive tomographic diagnostics, the discrepancy between the prevalence of aneurysms in the general population, which was estimated to be around 5–8% (62), and the incidence of SAH, which is around 11.3 per 100.000 person-years in Germany, increases, reflecting a benign behavior of most lesions (18, 50).

This raises critical questions about which patients with incidental findings should be treated and how to improve patient care.

Ideally, patients with incidental aneurysms are stratified into subcategories for identification of patients with high-risk aneurysms, who require a more aggressive management.

Although pathogenesis of intracranial aneurysms and of their rupture is intensively studied they are still poorly understood. Intracranial aneurysms derive from a multifactorial pathological process where environmental, genetic and hemodynamic factors play a role.

Anatomical variations are common findings during invasive and non-invasive diagnostic of posterior cerebral arterial circulation.

“Immature” variations of the distal basilar artery are commonly interpreted as benign conditions without pathological character, presenting only some implications during the treatment of concomitant neurovascular conditions due to the alteration of blood supply related to their presence.

In other portions of the circle of Willis, for instance ICA´s C6 segment, the presence of a fetal PComA is associated with a higher risk to develop a PComA aneurysm. Likewise, the presence of an ACoA aneurysm was related to distinct variant anatomical patterns like the presence of a dominant A1 or of a fenestration of the ACoA (52-59).

The goal of this study was to investigate, if anatomical variations of the distal basilar artery also play a role in the complex multifactorial process that results in the formation and rupture of an aneurysm in this location.

Furthermore, aneurysms originating from vessels with “immature” patterns were analyzed to determine if they harbor a more aggressive clinical behavior as compared to aneurysms originating from a “normal” vessel.

3 Materials und Methods

3.1 Data

In a retrospective study we analyzed patients with distal basilar artery aneurysms who were treated in the Neurosurgical Department of Heinrich Heine University, Düsseldorf between January 2000 and February 2017.

The information about patients' medical history and treatment were derived from discharge letters, outpatient´s clinic letters and operation reports that were available in our digital archive (Medico WMC, Siemens AG, Berlin, München).

Aneurysm morphological data were derived from computed tomography angiography (CTA), magnetic resonance angiography (MRA) and digital subtraction angiography (DSA) that are digitally saved and accessible via PACS (Sectra Medical Systems Linköping, Sweden). The study was approved by the Ethics Committee of the Heinrich-Heine-University (Study number: 5373).

3.2 Inclusion and exclusion criteria

Patients included in the study presented with an aneurysm originating from the basilar tip, from P1 segment of the PCA or from the s1 segment of the SCA and underwent CTA, MRA or DSA diagnostic imaging.

Aneurysms originating from basilar artery proximal to SCA´s origin or distal to P1 and s1 segments were excluded. Other exclusion criteria were patients without any imaging or with incomplete radiological diagnostics, for example MRI without MRA or indirect diagnosis of basilar tip aneurysm in a CT scan without contrast enhancement, seen as a mass in the interpeduncular cistern, and patients without sufficient medical records concerning bleeding and therapy. Aneurysms associated with arteriovenous malformations, pseudoaneuryms and mycotic aneurysms were excluded.

3.3 Parameters analyzed

Patient demographics were recorded including gender and age at aneurysm rupture, at occurrence of other non-rupture symptoms or at the time of diagnosis and therapy of asymptomatic lesions.

Aneurysm morphology was analyzed in each case, including dome size, neck size, dome-to-neck ratio (DNR), aspect ratio (AR), dome projection on the sagittal plane, and the presence of blebs (daughter sac) on the aneurysm (see Figure 3.3.1). The saccular or fusiform profile of the aneurysm was also recorded for P1 and s1 aneurysms.

Information concerning the type of treatment and the presence of concomitant aneurysms in other portions of intracranial circulation was also recorded.

The "evolutional" configuration of the distal basilar artery was analyzed in each case recording the presence of fetal PcomA, cranial, caudal or asymmetric fusion of the basilar tip. The angle between P1 and P2A segments was determined and qualitatively defined as normal or immature as described in paragraph 1.3. The incidence of developmental variations in the study population was compared to a randomly selected group of patients with intracranial aneurysm in a different location assumed to be homogeneous to the study population.

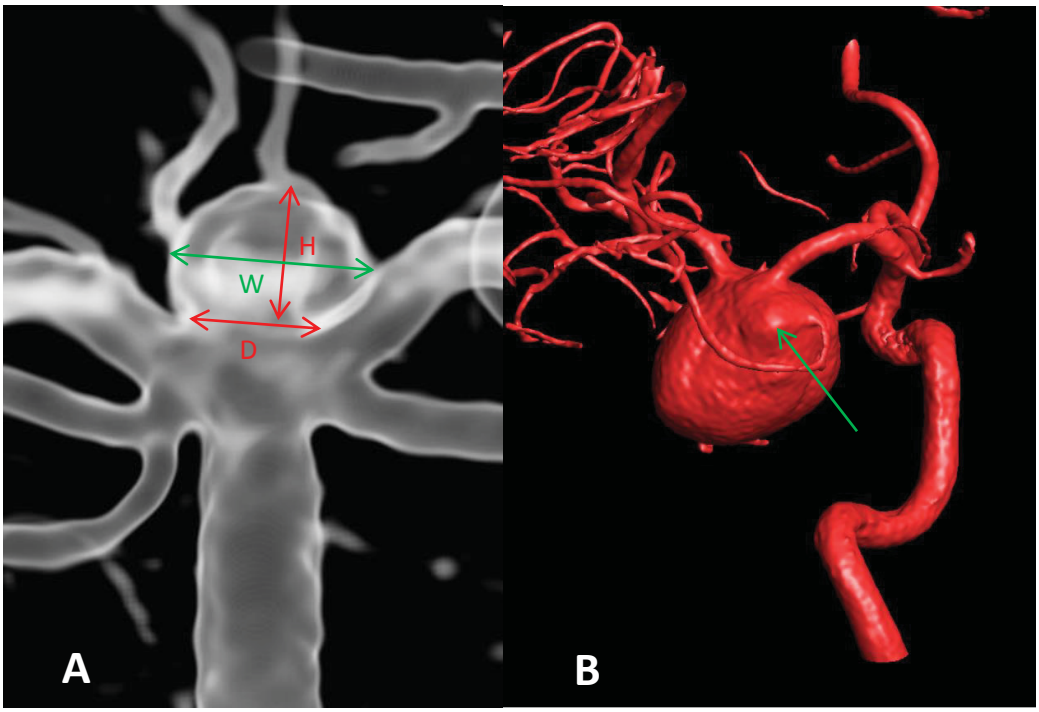

Figure 3.3.1: Panel A shows the principals of aneurysm measurements: perpendicular height (H), neck diameter (D), aneurysm width (W). Dome to neck ratio (DNR) corresponds to W/D, aspect ratio (AR) to H/D. The green arrow marks a bleb on this large left sided M1 aneurysm (B).

3.4 Interpretation of imaging diagnostics

The patients' digitally recorded radiological studies were visualized with PACS software, and data was derived from CTA, MRA, DSA images and 3D reconstruction of these. The measurements of the aneurysms and vessels were taken from the studies using appropriately calibrated measurement tools integrated in the software.

The visualization of the P1-P2 angle was derived from 3D models of the arterial system derived from CTA or MRA images.

3.5 Statistical analysis

After collection of the aforementioned parameters, they were defined in metric, ordinal and nominal scales and statistically analyzed with appropriate tests based on the type of data using SPSS Statistics (IBM Corp., Armonk, NY).

Demographic and clinical characteristics were analyzed for differences between study population and control group by use of the χ^2-test and 2-tailed t-test for binary and continuous variables, respectively. Morphologic aspects were studied using χ^2-test, Fisher's exact test and 2-tailed t-test.

All statistical analyses were 2-sided, and P value < 0.05 was considered statistically significant.

3.5.1 Chi-squared test

The Chi-Square test (X^2-test) is a non-parametric statistical test used to determine the agreement between the observed frequencies and the expected frequencies assuming the null hypothesis.

The result of a Chi-square analysis tells whether the difference is due to sampling error. The greater the deviation of what was observed to what was expected is, the greater the probability is that the difference is not due to chance.

Critical values for chi-square are sorted by degrees of freedom and probability levels. If the calculated chi-square value is greater than the critical value calculated, the null hypothesis is rejected.

3.5.2 Fisher's exact test

Fisher's exact test is a statistical significance test that is used in the analysis of contingency tables. Although in practice it is employed when sample sizes are small, it is valid for all sample sizes.

It is called exact test because the significance of the deviation from a null hypothesis (e.g., P-value) can be calculated exactly, rather than relying on an approximation that becomes exact in the limit as the sample size grows to infinity, as with many statistical tests.

3.5.3 Independent samples t-test

The t-test for independent-samples compares the means between two unrelated groups on the same continuous, dependent variable in order to determine whether there is statistical evidence that the associated population means are significantly different.

The Independent Samples t-test is a parametric test. With this test, each case must have scores on two variables, the grouping (independent) variable and the test (dependent) variable.

The grouping variable divides cases into two mutually exclusive groups or categories, while the test variable describes each case on some quantitative dimension such as test performance.

4 Results

4.1 Patient demographics

The population of patients treated for distal basilar artery aneurysms between January 2000 and February 2017 in the Neurosurgical Department of Heinrich Heine University, Düsseldorf comprised 95 patients with 101 aneurysms.

The mean age of the patients at the time of diagnosis was 53.6 ± 9.1 years, ranging from 33 to 84 years. The mean age at presentation was 53.3 ± 9.5 years for the patients with ruptured aneurysms and 53.3 ± 8.5 years for patients with incidental pathology.

The study population included 75 females (78.9%, mean age 53.4 ± 8.9 years) and 20 males (21.1%, mean age 54.2 ± 10.3 years). The mean age of patients with basilar tip aneurysm was lower (52.8 ± 8.8 years) than in patients with the pathology located in P1 and s1 segments (66.0 ± 9.9 years and 56.2 ± 10.0 years, respectively).

4.2 Aneurysm location

The aneurysm was located on the basilar tip in 69 patients (72.6%), on the s1 segment in 16 patients (16.8%) and on the P1 segment in 5 cases (5.3%).

The presence of multiple aneurysms was common in the study population as 46 of 95 patients (48.4%) presented with concomitant aneurysms, most occurring in other locations.

The presence of a second aneurysm in the distal basilar artery was observed in only 6 patients (6.3%). Five patients (5.3%) presented with one aneurysm on the basilar tip and another one on the s1 segment. One patient of the 5 patients with P1 aneurysms had 2 lesions located on the same P1 segment.

4.3 Aneurysm presentation

In most of the patients (63.1%, 60 individuals), the aneurysm in the distal basilar artery was diagnosed through emergency diagnostic after SAH, while the remaining 36.9% were an incidental finding. Most P1 (66.7%) and s1 aneurysms (76.2%) were not ruptured at presentation, whereas 73.0% of basilar tip lesions presented with SAH.

Amongst the 35 patients with intact aneurysms, only one patient, who had a P1 aneurysm, complained of symptoms related to the mass effect of the lesion.

4.4 Aneurysm treatment

Seventy-five patients (76.7%) of the study population were treated for 79 aneurysms. The majority of ruptured aneurysms (54 of 60) were treated. The remaining 10% were not treated due to poor neurological condition on admission or death prior to intervention. In the group of incidental lesions, 56.1% of the patients were treated.

The most common treatment option was endovascular coil embolization, which was performed in 55 aneurysms (71.4%), followed by stent assisted coiling in 20 cases (26.0%). One aneurysm (1.3%) was treated with a flow diverter and another one with microsurgical clipping.

In the subgroup of 62 treated basilar tip aneurysms, 42 aneurysms were coiled (67.7%), 19 were treated with stent assisted coiling (30.7%) and in one case a flow diverter was implanted (1.6%).

Of the three patients treated for P1 aneurysm, two (66.7%) were coiled and one (33,3%) underwent a stent assisted coiling.

In the subgroup of 21 s1 aneurysms, 14 were treated (66.6%). The majority was managed with coiling alone (78.6%), while two patients (14.3%) underwent stent assisted coiling and open surgery was performed in only one case (7.1%).

4.5 Aneurysm morphology

Concerning the morphology of basilar tip aneurysms, the mean width of the dome on the coronal plane and height on sagittal plane were 7.7 ± 4.8 mm and 6.8 ± 4.6 mm, respectively whereas the mean neck diameter was 4.6 mm ± 1.7 mm, resulting in a mean AR of 1.3 ± 0.6 and a DNR of 1.6 ± 1.2.

Ruptured basilar tip aneurysms presented with a wider and higher dome and thus larger AR compared to incidental lesions; however, none of these differences reached statistical significance (Table 4.1).

Basilar tip aneurysms presented with variable dome projections on the sagittal plane. In our series, a superior dome projection was most commonly encountered (79.9%), followed by anterior projections in 12.2% of cases. A posterior basilar tip aneurysm dome projection was reported in 4.1% of the pathology, while ventral-superior or superior-posterior projections were the least common morphology both encountered in only 1.4% of patients each.

In the subgroup of s1 aneurysms, the mean dome width on the coronal plane and the mean height on the z axis were 2.9 ± 1.7 mm and 3.2 ± 2.1 mm respectively. The mean neck diameter was 2.5 ± 1.1mm, resulting in a mean AR of 1.3 ± 0.5 and a dome neck ratio of 1.1 ± 0.3.

Morphological variations in dome width, height and AR in ruptured and unruptured s1 aneurysms were similar to those found amongst basilar tip aneurysm. Greater dome, width and AR were found in ruptured compared to unruptured cases (Table 4.1); however this difference was not statistically significant. On the other hand, the mean dome height in the ruptured group was significantly greater than that found in the incidental aneurysms (4.7 mm vs 2.9 mm, $P<0.01$).

While all basilar tip and s1 aneurysms were saccular, 33.3% of P1 aneurysms presented as fusiform lesions.

The mean dome width on the coronal plane and height on the sagittal plane of P1 aneurysms were 4.3 ± 2.9 mm and 4.4 ± 3.3 mm respectively. The mean AR of saccular lesions was 1.6 ± 1.2 and a mean dome neck ratio of 1.3 ± 0.6 was calculated.

In addition, although the ruptured P1 aneurysms had a greater dome width and height compared to unruptured lesions, this was not statistically significant (Table 4.1). AR could not be compared between these two groups due to low patient numbers and the presence of a fusiform pattern in 33% of cases.

Regarding the aneurysm dome morphology, blebs were present in 60% of P1 and 58.8% of basilar tip aneurysms, but in only 10% of s1 aneurysms. The presence of blebs was significantly more common in ruptured aneurysms of the distal basilar artery (61.8% of ruptured vs 28.9% of unruptured aneurysms, $P<0.01$).

		Ruptured			Unruptured			
		N =	Size (mm)	SD (mm)	N=	Size (mm)	SD (mm)	P=
Basilar tip aneurysms	Dome´s width	48	8.1	4.6	19	6.5	5.0	0.70
	Dome´s height	54	7.1	4.9	19	6.0	3.6	0.19
	Aspect ratio	49	1.3	0.6	17	1.2	0.4	0.29
s1 aneurysms	Dome´s width	4	3.6	2.3	16	2.7	1.6	0.19
	Dome´s height	4	4.7	3.5	16	2.9	1.5	**<0.01**
	Aspect ratio	4	1.6	0.8	16	1.2	0.4	0.11
P1 aneurysms	Dome´s width	2	4.7	3.7	4	4.2	3.0	0.75
	Dome´s height	2	7.1	4.0	4	3.1	2.5	0.38

Table 4.1: Comparison of the morphological variation of dome width, dome height and aspect ratio in ruptured and unruptured aneurysms of the basilar tip, s1 and P1. SD denotes standard deviation.

4.6 Distal basilar artery anatomy

We analyzed the morphology of the posterior circulation in our patient population with aneurysms in the distal basilar artery compared to a control group of patients with incidental or ruptured intracranial aneurysms in another location of intracranial circulation.

The morphology of the terminal portion of basilar artery was described as either a “mature” developmental fusion pattern or alternatively as immature by presence of caudal of asymmetric fusional morphologies. The control group as described in the material and methods (Section 3) included 68 patients.

The statistical analysis failed to demonstrate that the presence of a mature fusional pattern with symmetrical cranial fusion of bilateral longitudinal neural arteries is a “protective factor” against aneurysms on these arterial segments. As depicted in Table 4.2, an increased number of patients in the subgroup of patients with aneurysms in the distal basilar artery were noted to have an immature fusional pattern compared to the

expected distribution of frequencies; however, this was not statistically significant (Table 4.2, P=0.11).

The statistical analysis was repeated for each subgroup of patients according to the location of the aneurysm (basilar tip, s1 or P1). In the subpopulation of patients with basilar tip aneurysms, a higher frequency in the distribution was noted for the patients with immature fusion pattern as well as in the patients of the control group with mature fusion pattern (Table 4.2); however, the X^2-test did not demonstrate statistical significance for these results (P=0. 25).

In the subgroup of patients with s1 aneurysms, results were analogous to those described for basilar tip aneurysms, with a higher frequency of the immature basilar fusion pattern amongst patients with s1 aneurysms and of the mature fusion pattern in the control group. Yet, this difference was not statistically significant on the X^2-test (P=0.12).

Finally, analysis of the fusion pattern in the subpopulation of patients with P1 aneurysms revealed a higher frequency of patients with the immature fusion pattern and a P1 aneurysm as well as in the subpopulation of the control group with mature fusion pattern (Table 4.2). These results were not statistically significant by Fisher´s exact test.

		Mature fusional pattern			
		No	Yes	Test	P=
Distal basilar artery aneurysm	No	31/68	37/68	X^2	0.11
	Yes	48/82	34/82		
Basilar tip aneurysm	No	31/68	37/68	X^2	0.25
	Yes	36/65	29/65		
s1 aneurysm	No	31/68	37/68	X^2	0.12
	Yes	13/20	7/20		

P1 aneurysm	No	31	37	Fisher Exact	0.18
	Yes	4	1		

Table 4.2: The distribution of frequencies of morphological patterns in aneurysmal and non-aneurysmal patients for the distal basilar artery, the basilar tip, s1 and P1. Statistical significance was tested with appropriate test as given for each aneurysm location.

The fusion pattern of the distal basilar artery was also related to the AR of basilar tip aneurysms (Table 4.3); however, no statistically significant difference was identified.
In addition, there was no statistically significant correlation between the morphology of the distal basilar artery and the DNR of basilar tip aneurysms (Table 4.3) nor between the fusion pattern of the distal basilar artery and the presence of blebs on the dome in basilar tip aneurysms (Table 4.3).

The mean age of patients with ruptured basilar tip aneurysms was compared in two groups based on the fusion pattern of the distal basilar artery; however, the t-test did not show any statistically significant difference (Table 4.3).

		Mature fusional pattern				
		Yes	N=	No	N=	P=
Aspect ratio [mean (±SD)]		1.5 (±0.4)	27	1.5(±0.4)	31	0.97
Dome to neck ratio [mean (±SD)]		1.4(±0.4)	27	1.7(±1.6)	31	0.21
Age [mean years (±SD)]		49.4(±10.3)		53.4(±8.3)		0.15
Presence of blebs	Yes (N=34)	16		18		0.93
	No (N=27)	13		14		

Table 4.3: Mean aspect ratio, dome to neck ratio and patient age with standard deviation (SD) of basilar tip aneurysm in patients with mature and immature fusion patterns of the distal basilar artery showing no significant difference. Significance of difference was tested with Student's t-test with Levene's correction for unequal variances. Additionally, the frequencies of the presence of blebs are given depending on mature fusional pattern. Statistical significant was tested using X^2-test.

We further correlated the conformation of the P1-P2 junction to the presence of an aneurysm in the distal artery basilar. As described in the materials and methods (Section 3), the presence of an accentuated change of direction of the vessels between P1 and P2 segments was defined as an immature pattern. The analysis was initially performed in the whole aneurysmal population compared to the control group; 47.5% of aneurysms patients versus 40.8% of the control group presented an immature junction, however no significant correlation was observed in the statistical analysis (Table 4.4).

The presence of an embryological configuration of P1-P2 junction was further divided into unilateral or bilateral presence of this variation.

Table 4.4 shows the analysis performed for the subgroup with monolateral immature P1-P2 junction, which demonstrated no correlation between a monolateral immature P1-2 junction pattern and the presence of aneurysms in the distal basilar artery. A higher frequency of patients in the subgroup of individuals with distal basilar artery aneurysm compared to the control group was no significant. Similarly, no correlation was found between the occurrence of a distal basilar artery aneurysm and bilateral presence of an embryological P1-P2 junction (Table 4.4).

			Distal basilar artery aneurysm		
		N=	No	Yes	P=
Immature P1-P2 junction	No	84	42	42	0.36
	Yes	68	29	39	
Monolateral immature P1-P2 junction	No	95	48	47	0.23
	Yes	57	23	34	
Bilateral immature P1-P2 junction	No	139	65	74	0.96
	Yes	13	6	7	

Table 4.4: The distributions of frequencies of different P1-P2 junction morphologies in the subgroup of patients with distal basilar artery aneurysm and in the control group are given here. The X^2-test was used to identify significant differences in the distribution.

The presence of an immature pattern of the P1-P2 junction was also analyzed according to the occurrence of basilar tip, s1 segment and P1 segment aneurysms. As showed in Table 4.5, there was no statistically relevant asymmetry in the distribution of frequencies for patients with basilar tip aneurysms and immature P1-P2 junction morphology (P=0.60), nor amongst those with monolateral (P=0.41) or bilateral (P=0.61) variation.

			Basilar tip aneurysm		
		N=	No	Yes	P=
Immature P1-P2 junction	No	77	42	35	0.60
	Yes	58	29	29	
Monolateral immature P1-P2 junction	No	86	48	38	0.41
	Yes	49	23	26	
Bilateral immature P1-P2 junction	No	139	79	60	0.38
	Yes	13	9	4	

Table 4.5: The distributions of frequencies of different P1-P2 junction morphologies in the subgroup of patients with basilar tip aneurysm and in the control group are given here. The X^2-test was used to identify significant differences in the distribution.

Similarly amongst patients with s1 aneurysms, there was no association between the morphology of the P1-P2 junction and the presence of an aneurysm (Table 4.6).

			s1 aneurysm		
		N=	No	Yes	P=
Immature P1-P2 junction	No	52	42	10	0.61
	Yes	39	29	10	
Monolateral immature P1-P2 junction	No	60	48	12	0.59
	Yes	31	23	8	
Bilateral immature P1-P2 junction	No	82	65	17	0.38
	Yes	9	6	3	

Table 4.6: The distributions of frequencies of different P1-P2 junction morphologies in the subgroup of patients with s1 aneurysm and in the control group are given here. The X^2-test was used to identify significant differences in distribution.

Finally, all 5 patients with P1 aneurysms had monolateral immature P1-P2 junction morphology. The Fisher's exact test demonstrated statistical significance (P=0.01, Table 4.7).

			P1 aneurysm		
		N=	No	Yes	P=
Immature P1-P2 junction	No	42	42	0	0.01
	Yes	34	29	5	

Table 4.7: The distributions of frequencies of different P1-P2 junction morphologies in the subgroup of patients with s1 aneurysm and in the control group are given here. Fisher's exact test was used to identify significant differences in distribution.

The morphology of basilar tip aneurysms represented by diameter on the x, y and z axes, neck diameter, aspect ratio and DNR was compared between patients with mature

morphology of the P1-P2 junction and patients with immature junction morphology (Table 4.8). No relevant statistical correlation was noted.

	Immature P1-P2 junction morphology				
	Yes	N=	No	N=	P=
Diameter on X axis [mean mm (±SD)]	7.7 (±4.9)	27	6.8 (±3.9)	33	0.42
Diameter on Y axis [mean mm (±SD)]	7.9 (±4.6)	27	6.4 (±2.9)	33	0.15
Diameter on Z axis [mean mm (±SD)]	6.9 (±5.3)	27	6.8 (±3.3)	33	0.64
Neck´s diameter [mean mm (±SD)]	5.0 (±1.5)	25	4.4 (±1.9)	31	0.26
Aspect ratio [mean mm (±SD)]	1.4 (±0.4)	25	1.4 (±0.4)	31	0.96
Dome to neck ratio [mean mm (±SD)]	1.4 (±0.4)	25	1.7 (±1.6)	31	0.36

Table 4.8: The mean measurements in mm of basilar tip aneurysms on the x, y and z axes, the neck diameter, aspect ratio and dome to neck ratio are compared in the subgroup of patients with normal P1-P2 junction (No) and patients with junctional anomalies (Yes). The Student t-test with Levene's correction for unequal variances showed no statistical difference in the mean values.

Further investigations focused on the association between fetal morphology of PcomA and the presence of an aneurysm in the distal basilar artery. No correlation was shown (Table 4.9).

The analysis was repeated dividing the patients with distal basilar artery aneurysms into three groups according to the location of the aneurysm. Aneurysms at all three locations (basilar tip, s1 segment and P1 segment) showed no association with the morphology of the PComA (Table 4.9).

			Fetal PComA morphology			
		N=	No	Yes	Test	P=
Distal basilar artery aneurysm	No	73	46	27	X^2	0.12
	Yes	86	64	22		
Basilar tip aneurysm	No	73	46	27	X^2	0.10
	Yes	68	52	16		
s1 aneurysm	No	73	46	27	X^2	0.10
	Yes	21	13	8		
P1 aneurysm	No	73	46	27	Fisher Exact	1.00
	Yes	5	3	2		

Table 4.9: The distribution of frequencies of the fetal PComA morphology in patients with distal basilar aneurysms, basilar tip aneurysms, s1 aneurysms and P1 aneurysms and in the control group. Statistical significance was tested with appropriate test as given for each aneurysm location.

The presence of a duplication of SCA at the origin was analyzed according to the presence of s1 aneurysm; however, no statistically significant association was found (Table 4.10).

			s1 aneurysm		
		N=	No	Yes	P=
SCA duplication	No	111	96	15	0.68
	Yes	45	40	5	

Table 4.10: The distributions of frequencies of SCA duplication in the subgroup of patients with s1 aneurysm and in the control group are given here. The X^2-test was used to identify significant differences in distribution.

5 Discussion

5.1 Study population; demography, location, presentation and treatment of the aneurysms of distal basilar artery.

In our study we reviewed 95 patients with 101 aneurysms treated in the Neurosurgical Department of Heinrich Heine University, Düsseldorf between January 2000 and February 2017.

The aneurysms were mostly located on the basilar tip (72.6%) followed by s1 segment of superior cerebellar artery in 16.8% of patients. The less common site was the P1 segment of posterior cerebral artery which was involved in just 5.3%.

According to the literature, aneurysms of the vertebrobasilar system represent 10 to 18% of all intracranial aneurysms, and 50 to 65% of such lesions occur at the basilar bifurcation (18).

PCA aneurysms account for 1–2% of all intracranial aneurysms and conformingly to our series for 7% of all posterior circulation aneurysms (61). They are most commonly located in the P1 or P2 segments (100).

In the largest series of posterior circulation aneurysms treated by endovascular methods, the average age of these patients was 50.5 to 53.9 years and 59 to 72% were female, similar to the age and sex distributions seen in large studies of aneurysms of all intracranial locations (18-25).

The mean patients‘ age of 53.6 ± 9.1 and a female prevalence of 78.9% in our population correspond to the data reported in the literature.

The age at presentation didn´t differ among ruptured and unruptured aneurysms but patients with basilar tip lesions were younger compared to those with s1 or P1 pathology (respectively 52.8 ± 8.8 years, 66.0 ± 9.9 years, 56.2 ± 10.0 years).The reason for this difference is unknown.

The presence of another aneurysm was high in our study population. Among the 48.4% of patients with multiple lesions only 6.3% presented a second lesion in the distal basilar artery. The coexistence of a basilar tip and of an s1 aneurysm was observed in 5.3% of cases and one patient presented two lesions on the same P1 segment.

The literature reports an association of PCA aneurysms with multiple aneurysms and arteriovenous malformations (61).

Kaminogo et al. reported in a series of 2037 patients with SAH, 361 patients presenting with multiple aneurysms (60). In the study population the prevalence of a second aneurysm was higher compared to the 17.7% reported by above mentioned study. However the study by Kaminogo et al. holds several limitations. Due to poor neurological condition at admission 31.1% of the patients of this series did not undergo angiography and the sensibility of DSA was lower compared to modern 3D rotational sequences, especially during the first years of the study between 1989 and 1998, thus small aneurysms may have gone unnoticed.

Regarding symptoms at admission 63.1% of the patients presented with SAH from aneurysm rupture. In the largest series of posterior circulation aneurysms treated with endovascular techniques SAH is reported to be accordingly to our study the most common symptom at presentation with a variable incidence between 55 and 78% (18-25).

Only one patient suffering from a P1 aneurysm complained of symptoms related to the mass effect of the lesion. A relevant number of patients corresponding to 35.8% underwent diagnostics for symptoms not directly related to the pathology and were therefore diagnosed with an intact aneurysm. The above mentioned endovascular series report a quite similar incidence of unruptured asymptomatic lesions (14 to 31%).

In the subgroup of ruptured aneurysms 90% were treated, while 10% were not treated due to poor neurological condition on admission or death prior to intervention. 56.1% of the incidental aneurysms were treated.

The change from surgical to endovascular aneurysm treatment in our study population over time represents the paradigm shift in aneurysm treatment following the ISAT (33). Most of the patients corresponding to 71.4% were coiled while 26% underwent stent assisted coiling. Only one patient (1.3%) was treated with a flow diverter and another one with microsurgical clipping. A similar distribution of treatment modalities was encountered analyzing all 3 locations separately as described in the paragraph 4.4.

5.2 Aneurysm morphology

Basilar tip aneurysms were bigger compared to s1 and P1 lesions as demonstrated by a dome´s width and dome´s height of 7.7 ± 4.8 mm and 6.8 ± 4.6 mm respectively, compared to 2.9 ± 1.7 mm and 3.2 ± 2.1 mm for the s1 aneurysm group. The P1 group presented a dome´s width and dome´s height of 4.3 ± 2.9 mm and 4.4 ± 3.3 mm respectively.

In one study, the rank order for ruptured aneurysms according to aneurysm size in decreasing order was: ophthalmic, carotid bifurcation, basilar tip, MCA bifurcation, PcomA, AcoA, PICA and distal aneurysms (67). A similar study performed in the in the Korean population found the largest aneurysm on the basilar artery followed by MCA, ICA, and ACA.

Interestingly, the literature reports over 30% of PCA aneurysms to be large or giant, with tumor-like presentation. Giant aneurysms are defined by the Cooperative Study of Intracranial Aneurysms and Subarachnoid Hemorrhage as lesions with the largest diameter ≥ 2.5 cm (102). However our series analyzed only lesions located in P1 segment.

In all three anatomical locations ruptured lesions displayed larger AR compared to incidental lesions although the difference didn´t reach statistical significance probably due to the small sample size.

Carter et al. supposed that the aneurysm size at rupture may be determined by wall thickness and diameter of the parent vessel. According to Laplace's law which states that the tension required to withstand a given pressure increases with the diameter of a vessel, the critical diameter for rupture is proportional to the average wall thickness. This suggests that aneurysms at smaller arteries may rupture at smaller sizes since they initially had thinner walls (67).

The presence of blebs on the dome was significantly more common in ruptured aneurysms of the distal basilar artery compared to incidental lesions. Of ruptured lesions 61.8% compared to just 28.9% of unruptured aneurysms presented a bleb as a synonym for aneurysm wall instability. The difference reached statistical significance ($P<0.01$). Meng et al. demonstrated with a mathematical model based on Laplace´s law that the passive formation of a bleb in the weakest area of an aneurysm which reached the

stadium of imminent rupture represents initially a protection against rupture. The bleb initially decrease wall´s stress and then as it grows, this will increase again leading to rupture (104).

5.3 Correlation between aneurysms and anatomical variations

As known from other segments of the intracranial cerebral circulation, the presence of an alternative morphological pattern of a vessel may result in a different hemodynamic situation compared to the typical disposition and morphology of intracerebral arteries.

In the anterior circulation a hypoplasia of the A1 segment has been associated with the formation of AComA aneurysms, like the presence of a small A1–A2 angle junction (68, 69).

An analysis of the AComA region using computational flow dynamic techniques demonstrated that an asymmetrical ACom complex presents cross-flows and higher wall shear stress compared to a symmetric morphology. A resulting increased shear stress, between 5 to 10 times greater than the normal range, was believed to be related to the formation of AComA aneurysms (70).

Similar observations about the association between AComA morphology and the formation of an aneurysm are reported for the presence of a fenestration of the AComA or of an azygos artery instead of a paired A2 system (51-71).

Songsaeng et al. reported that AComA aneurysms are found more frequently together with A1 aplasia, followed by A1 hypoplasia and least commonly in a normally developed AComA complex (65).

These observations suggest that abnormal hemodynamic load derived by the presence of anatomical variations plays a particular role for the formation, growth and rupture of AComA aneurysms.

Similar reports postulated a correlation between a fetal morphology of PComA and the risk to develop a PcomA aneurysm (53, 61).

Starting from this assumption our study aimed to recognize the role of variations produced during the ontogenesis of this portion of the intracranial vascular three in the pathogenesis of intracranial aneurysms and of their course until rupture.

The study didn´t focus on the hemodynamic aspects correlated to the presence of one or another anatomical variation but on the observation of the incidence of these in our aneurysms population of the last 17 years.

As illustrated in the first section of this study, the distal basilar artery originates from the fusion of paired longitudinal neural arteries with branches from the dorsal division of the primitive carotid artery (2). Only after regression of the trigeminal artery and appearance of the vertebral artery, the basilar artery, due to its caudal-cranial directed process of fusion, acquires the definitive form where both s1 branches from the basilar trunk (5). Incomplete basilar artery fusion due to a stop in the maturation process produces a broad spectrum of immature configurations like fenestrations of the basilar artery or mono- or bilateral origin of the SCA from the PCA with various hemodynamic effects (2, 5, 8).

After inversion of the basilar artery flow from a centrifugal flow provided by the dorsal division of the carotid artery into a centripetal flow from the vertebral arteries a process of annexation ensues, capturing the posterior circulation, the telencephalic, diencephalic and rhombencephalic territories of the posterior division of the carotid artery.

This artery will regress to become the PComA and the P1-P2 junction will change its geometry under the influence of blood flow, as the P1 evolves from branch of the primitive PComA to mail feeder of P2 (2). The angle between P1-P2 will increase and then disappear, leaving a curved line.

Typical variations in the human population result from incomplete maturation in the ontogenesis of this portion of the cerebral vasculature. The presence of a fetal PComA represents a stop in the process of annexation of the PCA territory from P1 (2, 5). The persistence of a primitive P1 and P2A junction with or without concomitant presence of a fetal PComA corresponds to the original PComA-PCA arrangement in the embryonic life (2).

5.4 Aneurysms and distal basilar artery fusion pattern

Comparing the pattern of fusion of the distal basilar artery in the aneurysmal population with the control group we noted an increased number of patients with an immature fusional pattern corresponding to symmetric caudal or asymmetric fusion. Among 82

patients, where the fusional pattern could be recognized in the 3D reconstruction, 34 patients presented a mature pattern versus 48 that showed an immature form. The opposite was noted in the control group were 37 patients presented a traditional configuration and 31 some variation. This difference didn´t reach statistical relevance possibly due to the small sample size P=0.11.

The analysis was repeated dividing the patients in three groups according to the location of the pathology showing a predominance of an immature pattern in all subgroups (55.4% of basilar tip, 65% of s1 and 80% of P1 aneurysms) without statistical significance.

A report of Campos, where 47 consecutive basilar-tip aneurysms were reviewed showed that 9% of patients presented a cranial symmetrical fusion, 51% a caudal symmetrical and 39.8% an asymmetrical fusion (15). In the same work 47 normal basilar tips were compared to the aneurysmal group evidencing 30.4% cranial symmetrical, 26.1% caudal symmetrical and 43.5% asymmetrical disposition.

The data of Campos confirm the trend of our series, with a predominance of an immature fusional pattern in the patients with basilar tip aneurysms. In our analysis the control group showed the mature pattern as the most common pattern in 54.4% patients while in the study by Campos the most common pattern was the asymmetrical fusion. The discrepancies could be explained by different classification criteria, better visualization of the basilar tip with modern 3DRA or a difference between the populations analyzed.

The association between the fusion pattern and dome to neck ratio, AR, presence of blebs representing parameters of the aneurysm´s complexity and inclination to bleed respectively showed a slight higher presence of blebs and a greater DNR in the immature group without statistical significance, failing to demonstrate in our series, a role of fusion patters of distal BA in the multifactorial evolution of a new formed aneurysms into a big or complex one.

Comparing the age of the patients with basilar tip aneurysms at rupture, we observed no difference related to the fusional pattern excluding a more aggressive behavior of aneurysms growing from a basilar tip with immature morphology.

To our knowledge no study exists in the medical literature about the presence of anatomical variations of this or of other portions of intracranial arterial circulation like PcomA and AComA and the age at presentation of an aneurysm.

5.5 Aneurysms and morphology of P1-P2 junction

The correlation between morphology of the P1-P2 junction and the presence of an aneurysm in the distal basilar artery was initially performed considering the whole aneurysmal population. A difference was noted with 40.8% of the control group presenting an immature junction compared to 48.1% in the aneurysm patients; however this was statistically not significant.

A separated subanalysis showed similar results for patients with unilateral presence of an immature junction with 42% of patients in the aneurysm group versus 32.4% in the control group. Probably the small sample size explains the lack of statistical relevance of the results (P=0.22). The same analysis in patients with bilateral junction showed no asymmetric distribution in the group of 13 patients.

The influence of the junction´s morphology was analyzed for each aneurysm location. All five patients with P1 aneurysm showed a monolateral immature P1-P2A junction on angiogram. In four patients the anomaly was ipsilateral of the lesion and interestingly only one of these patients presented a fetal PComA on the side of the aneurysm. In one patient the ipsilateral junction was not visualized due to the presence of the complex fusiform aneurysm and the contralateral side presented a junctional anomaly. The analysis confirmed a statistical relevance of the results (P=0.01).

The hemodynamic effect of an acute direction change in the P1-P2A junction when P2 is not fed by a fetal PComA is obvious, as it produces more turbulence compared to an artery with a linear or curvilinear course. However, here the side of aneurysm formation in not the P1-P2A junction but the more proximal P1 junction where the increased hemodynamic stress due to morphology of the junction is not present because of flow orientation being the P1 segment proximal to the junction. As postulated by Lasjaunias (2) this may suggest the presence of other concomitant alterations related to an embryonal morphology which renders the artery prone to form an aneurysm maybe due to an immature constitution of the arterial wall.

The influence of the morphology of P1-P2 junction on basilar tip and s1 aneurysms is reflected in 45.3% of basilar tip aneurysms having an embryological configuration compared to 40.8% of the control group and 50% of the patients with s1 aneurysm having an embryological configuration compared to 40.8% in the control group. The subanalysis, dividing the presence of the anatomical variation into monolateral and bilateral, confirmed the results with exception of the small group of four patients with basilar tip aneurysm. None of these calculations was statistically relevant.

The size of basilar tip aneurysm, aspect and dome neck ratio was also compared to the presence of an immature P1-P2 junction. No relevant statistical correlation was noted.

The last analysis regarded the presence of fetal PComA morphology where an association with the presence of an aneurysm was excluded in all groups.

6 Conclusions:

The presence of an immature P1-P2A junction should be considered as risk factor for aneurysms on the P1 segment of the PCA. The reasons for this correlation remain obscure and have probably to be searched in the vessel wall of this embryological immature arterial segment. Multicenter trials are required to collect a bigger patient´s sample to confirm the role of the P1-P2A junction in s1 and basilar tip aneurysms and to elucidate the impact of immature fusion patterns of the distal basilar artery.

References

1. Klosovskii BN. The development of the brain and its disturbance by harmful factors. Macmillan Company, 1963

1. Stoeter P, Drews V. Vorgeburtliche Entwicklung der Hirnvenen und Sinus mit Varianten und Dysplasien. **Radiologie 23:**273-283

2. Lasjaunias PL, Ter Brugge KG, Berenstein A. Surgical Neuroangiography: Clinical Vascular Anatomy and Variations, 2nd ed. Springer-Verlag, 2001

3. Dungan DH, Heiserman JE. The carotid artery: embryology, normal anatomy, and physiology. **Neuroimaging Clin N Am 6:**789–799, 1996

4. Raybaud C. Normal and abnormal embryology and development of the intracranial vascular system. **Neurosurg Clin N Am 21:**399-426, 2010

5. Padget DH. The development of the Cranial Arteries in the Human Embryo. **Carnegie Institution 32:**205-261, 1948

6. Shapiro M. http://neuroangio.org/neurvascular-evolution/, 2018

7. Larsen WJ. Human Embryology. Churchill Livingstone, 1997

8. Rhoton AL Jr. Rhoton's Cranial Anatomy and Surgical Approaches. Lippincott, Williams and Wilkins, 2007

9. Marinkovic S, Gibo H.The surgical anatomy of the perforating branches of the basilar artery. **Neurosurgery 33:**80–87, 1993

10. Saeki N, Rhoton AL Jr: Microsurgical anatomy of the upper basilar artery and the posterior circle of Willis. **J Neurosurg 46:**563–578, 1977

11. Sufianov AA, Sufianova GZ, Iakimov IA. Microsurgical study of the interpeduncular cistern and its communication with adjoining cisterns. **Childs Nerv Syst 25:**301-8, 2009

12. Zeal AA, Rhoton AL Jr: Microsurgical anatomy of the posterior cerebral artery. **J Neurosurg 48:**534–559, 1978.

13. Stephens RB, Stilwell DL: Arteries and Veins of the Human Brain. CC Thomas, 1969.

14. Campos C, Churojana A, Rodesch G, Alvarez H, Lasjaunias P. Basilar tip aneurysm and basilar tip anatomy. **Intervent Neuroradio l4:**121-125, 1998

15. Adachi B. Das Arteriensystem der Japaner, vol I. Maruzen, 1928

16. van Raamt AF, Mali WP, van Laar PJ, van der Graaf Y. The fetal variant of the circle of Willis and its influence on the cerebral collateral circulation. **Cerebrovasc Dis 22:**217–224, 2006

17. Spetzler RF, Yashar M, Kalani S, Nakaji P. Neurovascular Surgery 2nd Edition, Thieme, 2015

18. Bavinzski G, Killer M, Gruber A, Reinprecht A, Gross CE, Richling B. Treatment of basilar artery bifurcation aneurysms by using Guglielmi detachable coils: a 6-year experience. **J Neurosurg 90:**843–852, 1999

19. Eskridge JM, Song JK. Endovascular embolization of 150 basilar tip aneurysms with Guglielmi detachable coils: results of the Food and Drug administration multicenter clinical trial. **J Neurosurg 89:**81–86, 1998

20. Guglielmi G, Viñuela F, Duckwiler G, et al. Endovascular treatment of posterior circulation aneurysms by electrothrombosis using electrically detachable coils. **J Neurosurg 77:**515–524, 1992

21. Lempert TE, Malek AM, Halbach VV, et al. Endovascular treatment of ruptured posterior circulation cerebral aneurysms. Clinical and angiographic outcomes. **Stroke 31:**100–110, 2000

22. Lozier AP, Connolly ES Jr, Lavine SD, Solomon RA. Guglielmi detachable coil embolization of posterior circulation aneurysms: a systematic review of the literature. **Stroke 33:**2509–2518, 2002

23. Mordasini P, Schroth G, Guzman R, Barth A, Seiler RW, Remonda L. Endovascular treatment of posterior circulation cerebral aneurysms by using Guglielmi detachable coils: a 10-year single-center experience with special regard to technical development. **AJNR Am J Neuroradiol 26:**1732–1738, 2005

24. Pandey AS, Koebbe C, Rosenwasser RH, Veznedaroglu E. Endovascular coil embolization of ruptured and unruptured posterior circulation aneurysms: review of a 10-year experience. **Neurosurgery 60:**626–636, 2007

25. Peluso JP, van Rooij WJ, Sluzewski M, Beute GN. Coiling of basilar tip aneurysms: results in 154 consecutive patients with emphasis on recurrent haemorrhage and re-treatment during mid- and long-term follow-up. **J Neurol Neurosurg Psychiatry 79:**706–711, 2008

26. Brinjikji W, Zhu YQ, Lanzino G, Cloft HJ, Murad MH, Wang Z et al: Risk factors for growth of intracranial aneurysms: A systematic review and meta-analysis. **AJNR Am J Neuroradiol 37:**615-620, 2016

27. Cebral JR, Sheridan M, Putman CM: Hemodynamics and bleb formation in intracranial aneurysms: **AJNR Am J Neuroradiol 31:**304-310, 2010

28. Wermer MJ, van der Schaaf IC, Algra A, Rinkel GJ. Risk of rupture of unruptured intracranial aneurysms in relation to patient and aneurysm characteristics: an updated meta-analysis. **Stroke 38:**1404–1410, 2007

29. Flemming KD, Wiebers DO, Brown RD Jr, et al. Prospective risk of hemorrhage in patients with vertebrobasilar nonsaccular intracranial aneurysm. **J Neurosurg 101:**82–87, 2004

30. Flemming KD, Wiebers DO, Brown RD Jr, et al. The natural history of radiographically defined vertebrobasilar nonsaccular intracranial aneurysms. **Cerebrovasc Dis 20:**270–279, 2005

31. Schievink WI. Intracranial aneurysms. **N Engl J Med 336:**28–40, 1997

32. Anson JA, Lawton MT, Spetzler RF. Characteristics and surgical treatment of dolichoectatic and fusiform aneurysms. **J Neurosurg 84:**185–193, 1996

33. Molyneux A, Kerr R, Stratton I, Sandercock P, Clarke M, Shrimpton J, Holman R; International Subarachnoid Aneurysm Trial (ISAT), Collaborative Group. International Subarachnoid Aneurysm Trial (ISAT) of neurosurgical clipping versus endovascular coiling in 2143 patients with ruptured intracranial aneurysms: a randomised trial. **Lancet 360:**1267-74, 2002

34. Fernandez Zubillaga A, Guglielmi G, Viñuela F, Duckwiler GR. Endovascular occlusion of intracranial aneurysms with electrically detachable coils: correlation of aneurysm neck size and treatment results. **AJNR Am J Neuroradiol 15:**815–820, 1994

35. Lefkowitz MA, Gobin YP, Akiba Y, et al. Balloon-assisted Guglielmi detachable coiling of wide-necked aneurysms: part II clinical results. **Neurosurgery 45:**531–537, 1999

36. Chow MM, Woo HH, Masaryk TJ, Rasmussen PA. A novel endovascular treatment of a wide-necked basilar apex aneurysm by using a Y-configuration, double-stent technique. **Am J Neuroradiol 25:**509–512, 2004

37. Fargen KM, Mocco J, Neal D, et al. A multicenter study of stent-assisted coiling of cerebral aneurysms with a Y configuration. **Neurosurgery 73:**466–472, 2013

38. Dalyai RT, Randazzo C, Ghobrial G, et al. Redefining Onyx HD 500 in the flow diversion era. **Int J Vasc Med 2012:**435490, 2012

39. Fiorella D, Kelly ME, Albuquerque FC, Nelson PK. Curative reconstruction of a giant midbasilar trunk aneurysm with the pipeline embolization device. **Neurosurgery 64:**212–217, 2009

40. Siddiqui AH, Abla AA, Kan P, et al. Panacea or problem: flow diverters in the treatment of symptomatic large or giant fusiform vertebrobasilar aneurysms. **J Neurosurg 116:**1258–1266, 2012

41. Lawton MT. Seven Aneurysms: Tenets and Techniques for Clipping. Thieme, 2010

42. Drake CG, Peerless SJ, Hernesniemi J. Surgery of Vertebrobasilar Aneurysms. Springer-Verlag, 1996

43. Yaşargil MG. Microneurosurgery, vol. 2. Thieme-Stratton, 1984

44. Yaşargil MG. Microneurosurgery, vol 1. Thieme-Stratton, 1984

45. International Study of Unruptured Intracranial Aneurysms Investigators. Unruptured intracranial aneurysms risk of rupture and risks of surgical intervention. **N Engl J Med 339:**1725–1733, 1998

46. Dolenc VV, Skrap M, Sustersic J, Skrbec M, Morina A. A transcavernous transsellar approach to the basilar tip aneurysms. **Br J Neurosurg 1:**251–259, 1987

47. Hernesniemi J, Ishii K, Niemelä M, Kivipelto L, Fujiki M, Shen H. Subtemporal approach to basilar bifurcation aneurysms: advanced technique and clinical experience. **Acta Neurochir Suppl (Wien) 94:**31–38, 2005

48. Sugita K, Kobayashi S, Shintani A, Mutsuga N. Microneurosurgery for aneurysms of the basilar artery. **J Neurosurg 51:**615–620, 1979

49. van Lieshout JH, Fischer I, Kamp MA, Donders ART, Cornelius JF, Steiger HJ, Boogaarts HD, Petridis AK. Subarachnoid Hemorrhage in Germany Between 2010 and 2013: Estimated Incidence Rates Based on a Nationwide Hospital Discharge Registry. **World Neurosurg 104:**516-521, 2017

50. Brismar J. Persistent hypoglossal artery, diagnostic criteria. Report of a case. **Acta Radiol Diagn (Stockh) 17:**160-166, 1976

51. Can A, Ho AL, Emmer BJ, Dammers R, Dirven CM, Du R. Association Between Vascular Anatomy and Posterior Communicating Artery Aneurysms. **World Neurosurg 84:**1251-5, 2015

52. Can, A. Mouminah, AL. Ho, Du R. Effect of vascular anatomy on the formation of basilar tip aneurysms. **Neurosurgery 76:**62-66, 2015

53. Cebral JR, Mut,F, Weir J, Putman C. Quantitative characterization of the hemodynamic environment in ruptured and unruptured brain aneurysms. **AJNR Am J Neuroradiol 32:**145-151, 2011

54. F.T. Charbel, D. Seyfried, B. Mehta, M. Dujovny, J.I. AusmanDominant A1: angiographic and clinical correlations with anterior communicating artery aneurysms **Neurol Res 13:**253-256, 1991

55. Flores BC, Scott WW, Eddleman CS, Batjer HH, Rickert KL. The A1-A2 diameter ratio may influence formation and rupture potential of anterior communicating artery aneurysms. **Neurosurgery 73:**845-853, 2013

56. Ingebrigtsen T, Morgan, Faulder K, Ingebrigtsen L, Sparr T, Schirmer H. Bifurcation geometry and the presence of cerebral artery aneurysms. **J Neurosurg 101:**108-113, 2004

57. Kasuya H, Shimizu T, Nakaya N, Sasahara A, Hori T, Takakura T. Angles between A1 and A2 segments of the anterior cerebral artery visualized by three-dimensional

computed tomographic angiography and association of anterior communicating artery aneurysms. **Neurosurgery 45:**89-93, 1999

58. Kim DW, Kang SD. Association between internal carotid artery morphometry and posterior communicating artery aneurysm. **Yonsei Med J 48:**634-638, 2007

59. Kaminogo M1, Yonekura M, Shibata S. Incidence and outcome of multiple intracranial aneurysms in a defined population. **Stroke 34:**16-21, 2003

60. Cebral JR Raschi M. Suggested Connections between Risk Factors of Intracranial Aneurysms: A Review. **Ann Biomed Eng 41:**1366–1383, 2013

61. Rinkel GJ, Djibuti M, Algra A, van Gijn J. Prevalence and risk of rupture of intracranial aneurysms: a systematic review. **Stroke 29:**251-6, 1998

62. Sato K, Yoshimoto Y. Risk profile of intracranial aneurysms: rupture rate is not constant after formation. **Stroke 42:**3376-81, 2011

63. Sforza DM, Putman CM, Cebral JR. Hemodynamics of Cerebral Aneurysms. **Annu Rev Fluid Mech 41:**91-107, 2009

64. Songsaeng D, Geibprasert S, Willinsky R, Tymianski M, TerBrugge KG, Krings T. Impact of anatomical variations of the circle of Willis on the incidence of aneurysms and their recurrence rate following endovascular treatment. **Clin Radiol 65:**895-901, 2010

65. Seoane ER, Tedeschi H, de Oliveira E, Siqueira MG, Calderón GA, Rhoton AL Jr. Management strategies for posterior cerebral artery aneurysms: a proposed new surgical classification. **Acta Neurochir (Wien) 139:**325-31, 1997

66. Carter BS, Sheth S, Chang E, Sethl M, Ogilvy CS. Epidemiology of the Size Distribution of Intracranial Bifurcation Aneurysms: Smaller Size of Distal Aneurysms and Increasing Size of Unruptured Aneurysms with Age. **Neurosurgery 58:**217–223, 2006

67. Kwak R, Ohi T, Niizuma H, Suzuki J. Relationship between the Afferent Artery and the Site of Neck of Anterior Communicating Artery Aneurysm, and Hemodynamics in the Anterior Part of the Circle of Willis. **No Shinkei Geka 6:**1159–1163, 1978

68. Kasuya H, Shimizu T, Nakaya K, Sasahara A, Hori T, Takakura K. Angeles between A1 and A2 Segments of the Anterior Cerebral Artery Visualized by Three-Dimensional Computed Tomographic Angiography and Association of Anterior Communicating Artery Aneurysms. **Neurosurgery 45:**89–93, 1999

69. Ujiie H, Liepsch DW, Goetz M, Yamaguchi R, Yonetani H, Takakura K: Hemodynamic Study of the Anterior Communicating Artery. **Stroke 27:**2086–2093, 1996

70. Baldawa S, Katikar D, Marda S. Giant saccular distal azygos artery aneurysm: Report of a case and review of literature. **Asian J Neurosurg 11:**175, 2016

71. Mackey J, Brown RD, Moomaw Jr CJ, Sauerbeck J, Hornung R, Gandhi D, Woo D, Kleindorfer D, Flaherty DL, Meissner I, Anderson C, Connolly ES, Rouleau G, Kallmes DF, Torner J, Huston J, Broderick JP, FIA and ISUIA Investigators. Unruptured intracranial aneurysms in the Familial Intracranial Aneurysm and International Study of Unruptured Intracranial Aneurysms cohorts: differences in multiplicity and location. **J Neurosurg 117:**60-64, 2012

72. Woodcock RJ, Cloft HJ, Dion JE. Bilateral type 1 proatlantal arteries with absence of vertebral arteries. **AJNR Am J Neuroradiol 22:**418-420, 2001

73. Okahara M, Kiyosue H, Mori H, Tanoue S, Sainou M, Nagatomi H. Anatomic variations of the cerebral arteries and their embryology: a pictorial review. **Eur Radiol 12:**2548-2561, 2002

74. Teal JS, Rumbaugh CL, Bergeron RT, Segall HD. Angio¬graphic demonstration of fenestrations of the intradural intra¬cranial arteries. **Radiology 106:**123-126, 1973

75. Vasović L, Trandafilović M, Jovanović I, Ugrenović S, Antović A, Karadžić R, et al. Human basilar artery abnormalities in the prenatal and postnatal period. **World Neurosurg 79:**15-23, 2013

76. Caldemeyer KS, Carrico JB, Mathews VP. The radiology and embryology of anomalous arteries of the head and neck. **AJR Am J Roentgenol 170:**197-203, 1998

77. Yilmaz E, Ilgit E, Taner D. Primitive persistent carotid-basilar and carotid-vertebral anastomoses: a report of seven cases and a review of the literature. **Clin Anat 8:**36-43, 1995

78. Sahni D, Jit I, Lal V. Variations and anomalies of the posterior communicating artery in Northwest Indian brains. **Surg Neurol 68:**449-453, 2007

79. Saltzman GF. Patent primitive trigeminal artery studied by cerebral angiography. **Acta Radiol 51:**329-336, 1959

80. McKenzie JD, Dean BL, Flom RA. Trigeminal-cavernous fistula: Saltzman anatomy revisited. **AJNR Am J Neuroradiol 17:**280-282, 1996

81. Ronkainen A, Hernesniemi J, Puranen M, et al. Familial intracranial aneurysms. **Lancet 349:**380-384, 1997

82. Lin N, Ho A, Gross BA, et al. Differences in simple morphological variables in ruptured and unruptured middle cerebral artery aneurysms. **J Neurosurg 117:**913-919, 2012

83. Ho AL, Mouminah A, Du R. Posterior cerebral artery angle and the rupture of basilar tip aneurysms. **PLoS One. 9:**e110946, 2014

84. Raphaeli G, Bandeira A, Mine B, Brisbois D, Lubicz B. A rare variant of persistent trigeminal artery: cavernous carotid-cerebellar artery anastomosis: a case report and a systematic review. **Cerebellum 8:**445-447, 2009.

85. Ali S, Radaideh MM, Shaibani A, Russell EJ, Walker MT. Persistent trigeminal artery terminating in the posterior inferior cerebellar artery: case report. **Neurosurgery 62:**746-8, 2008

86. Rennert J, Ullrich WO, Schuierer G. A rare case of supraclinoid internal carotid artery (ICA) fenestration in combination with duplication of the middle cerebral artery (MCA) originating from the ICA fenestration and an associated aneurysm. **Clin Neuroradiol 23:**133-136, 2013

87. Finlay HM, Canham PB. The layered fabric of cerebral artery fenestrations. **Stroke 25:**1799-1806, 1994

88. Sanders WP, Sorek PA, Mehta BA. Fenestration of intracranial arteries with special attention to associated aneurysms and other anomalies. **AJNR Am J Neuroradiol 14:**675-680, 1993

89. Farnoush A, Qian Y, Avolio A. Effect of inflow on computational fluid dynamic simulation of cerebral bifurcation aneurysms. **Conf Proc IEEE Eng Med Biol Soc. 2011:**1025-8

90. Hademenos GJ, Massoud TF. The Physics of Cerebrovascular Diseases: Biophysical mechanisms of development, diagnosis, and therapy. Springer, 1998

91. Padget DH. The circle of Willis: its embryology and anatomy. In: Dandy WE. Intracranial Arterial Aneurysm. Comstock, 1945

92. Polguj M, Podgórski M, Jędrzejewski K, Topol M, Majos A. Fenestration and duplication of the vertebral artery: the anatomical and clinical points of view. **Clin Anat 26:**933-943, 2013

93. Parmar H, Sitoh YY, Hui F. Normal variants of the intracranial circulation demonstrated by MR angiography at 3T. **Eur J Radiol 56:**220-228, 2005

94. Lesley WS, Dalsania HJ. Double origin of the posterior inferior cerebellar artery. **AJNR Am J Neuroradiol 25:**425-427, 2004

95. Hudák I, Lenzsér G, Lunenkova V, Dóczi T. Cerebral arterial fenestrations: a common phenomenon in unexplained sub¬arachnoid haemorrhage. **Acta Neurochir (Wien) 155:**217-222, 2013

96. Alpers BJ, Berry RG, Paddison RM. Anatomical studies of the circle of Willis in normal brain. **AMA Arch Neurol Psychiatry 81:**409-418, 1959

97. Gutierrez J, Sultan S, Bagci A, Rundek T, Alperin N, Elkind MS, et al. Circle of Willis configuration as a determinant of intracranial dolichoectasia. **Cerebrovasc Dis 36:**446-453, 2013

98. Chimowitz MI, Lynn MJ, Howlett-Smith H, Stern BJ, Hertzberg VS, Frankel MR, et al. Comparison of warfarin and aspirin for symptomatic intracranial arterial stenosis. **N Engl J Med 352:**1305-1316, 2005

99. Sacco RL, Kargman DE, Gu Q, Zamanillo MC. Race-ethnicity and determinants of intracranial atherosclerotic cerebral infarction. The Northern Manhattan Stroke Study. **Stroke 26:**14-20, 1995

100. Ciceri EF, Klucznik RP, Grossman RG, Rose JE, Mawad ME. Aneurysms of the Posterior Cerebral Artery: Classification and Endovascular Treatment. **American Journal of Neuroradiology January 22**;27-34, 2001

101. Alastruey J, Parker KH, Peiró J, Byrd SM, Sherwin SJ. Modelling the circle of Willis to assess the effects of anatomical variations and occlusions on cerebral flows. **J Biomech 40:**1794-1805, 2007

102. Locksley HB. Natural history of subarachnoid hemorrhage, intracranial

aneurysms and arteriovenous malformations. Based on 6368 cases in the cooperative study. **J Neurosurg 25:**219–239, 1966

103. El-Barhoun EN, Gledhill SR, Pitman AG. Circle of Willis artery diameters on MR angiography: an Australian reference database. **J Med Imaging Radiat Oncol 53:**248-260, 2009

104. Meng H, Feng Y, Woodward SH, Bendok BR, Hanel RA, Guterman LR, Hopkins LN. Mathematical model of the rupture mechanism of intracranial saccular aneurysms through daughter aneurysm formation and growth. **Neurol Res 27:**459–465, 2005

105. Glasscock ME 3rd, Seshul M, Seshul MB Sr. Bilateral aberrant internal carotid artery case presentation. **Arch Otolaryngol Head Neck Surg 119:**335-339, 1993

106. Silbergleit R, Quint DJ, Mehta BA, Patel SC, Metes JJ, Noujaim SE. The persistent stapedial artery. **AJNR Am J Neuroradiol 21:**572-577, 2000

107. Kathuria S, Gregg L, Chen J, Gandhi D. Normal cerebral arterial development and variations. **Semin Ultrasound CT MR 32:**242-251, 2011

108. Gumus T, Onal B, Ilgit ET. Bilateral persistence of type 1 proatlantal arteries: report of a case and review of the literature. **AJNR Am J Neuroradiol 25:**1622-1624, 2004

109. Willinsky R, Lasjaunias P, Berenstein A. Intracavernous branches of the internal carotid artery (ICA). Comprehensive review of their variations. **Surg Radiol Anat 9:**201-215, 1987

110. Jacobsson M, Davidsson A, Hugosson S, Tjellström A, Svendsen P. Aberrant intratympanic internal carotid artery: a potentially hazardous anomaly. **J Laryngol Otol 103:**1202-1205, 1989

111. Lasjaunias P, Moret J, Manelfe C, Théron J, Hasso T, Seeger J. Arterial anomalies at the base of the skull. **Neuroradiology 13:**267-272, 1977

112. Maiuri F, Donzelli R, de Divitiis O, Fusco M, Briganti F. Anomalous meningeal branches of the ophthalmic artery feeding meningiomas of the brain convexity. **Surg Radiol Anat 20:**279-284, 1998

113. Daseler EH, Anson BJ. Surgical anatomy of the subclavian artery and its branches. **Surg Gynecol Obstet 108:**149-174, 1959

114. Van Overbeeke JJ, Hillen B, Tulleken CA. A comparative study of the circle of Willis in fetal and adult life. The configuration of the posterior bifurcation of the posterior communicating artery. **J Anat 176:**45-54, 1991

115. Chen CJ, Chen ST, Hsieh FY, Wang LJ, Wong YC. Hypoplasia of the internal carotid artery with intercavernous anastomosis. **Neuroradiology 40:**252-254, 1998

116. Watanabe T, Togo M. Accessory middle cerebral artery. Report of four cases. **J Neurosurg 41:**248-251, 1974

117. Ravensbergen J, Krijger JK, Hillen B, Hoogstraten HW. The influence of the angle of confluence on the flow in a vertebro-basilar junction model. **J Biomech 29:**281-299, 1996

118. Moret J, Delvert JC, Bretonneau CH, Lasjaunias P, de Biĉetre CH. Vascularization of the ear: normal-variations-glomus tumors. **J Neuroradiol 9:**209-260, 1982

119. Manninen H, Mäkinen K, Vanninen R, Ronkainen A, Tulla H. How often does an incomplete circle of Willis predispose to cerebral ischemia during closure of carotid artery? Postmortem and clinical imaging studies. **Acta Neurochir (Wien) 151:**1099-1105, 2009

120. Yu M, Huang Q, Hong B, Qiao F, Liu J. Morphological differences between the aneurysmal and normal artery in patients with internal carotid-posterior communicating artery aneurysm. **J Clin Neurosci 17:**1395-1398, 2010

121. Vlak MH, Algra A, Brandenburg R, Rinkel GJ. Prevalence of unruptured intracranial aneurysms, with emphasis on sex, age, comorbidity, country, and time period: a systematic review and meta-analysis. **Lancet Neurol 10:**626-636, 2011

122. Crompton MR. The pathology of ruptured middle-cerebral aneurysms with special reference to the differences between the sexes. **Lancet 2:**421-425, 1962

123. Teal JS, Rumbaugh CL, Bergeron RT, Segall HD. Anomalies of the middle cerebral artery: accessory artery, duplication, and early bifurcation. **Am J Roentgenol Radium Ther Nucl Med 118:**567-575, 1973

124. Caruso G, Vincentelli F, Rabehanta P, Giudicelli G, Grisoli F. Anomalies of the P1 segment of the posterior cerebral artery: early bifurcation or duplication, fenestration, common trunk with the superior cerebellar artery. **Acta Neurochir (Wien) 109:**66-71, 1991

125. Sing PK, Marzo A, Howard B, Rufenacht DA, Bijlenga P, Frangi AF, Lawford PV, Coley SC, Hose DR, Patel UJ. Effects of smoking and hypertension on wall shear stress and oscillatory shear index at the site of intracranial aneurysm formation. **Clin Neurol Neurosurg, 112:**306-313,2010

126. Tarulli E, Fox AJ. Potent risk factor for aneurysm formation: termination aneurysms of the anterior communicating artery and detection of A1 vessel asymmetry by flow dilution. **AJNR Am J Neuroradiol 31**:1186-1191, 2010

127. Tomsick TA, Lukin RR, Chambers AA. Persistent trigeminal artery: unusual associated abnormalities. **Neuroradiology 17:**253-257, 1979

128. Geibprasert S, Pongpech S, Armstrong D, Krings T. Dangerous extracranial–intracranial anastomoses and supply to the cranial nerves: vessels the neurointerventionalist needs to know. **AJNR Am J Neuroradiol 30:**1459-1468, 2009

129. Okuno T, Nishiguchi T, Hayashi S, Miyamoto K, Terashita T, Itakura T, et al. A case of carotid superior cerebellar artery anastomosis associated with bilateral hypoplasia of the

internal carotid artery represented as the rupture of posterior cere-bral artery-posterior communicating artery aneurysm. **No Shinkei Geka 16:**1211-1217, 1988

130. Gibbons GH, Dzau VJ. The emerging concept of vascular remodeling. **N Engl J Med 330:**1431-1438, 1994

131. Plate KH. Mechanisms of angiogenesis in the brain. **J Neuropathol Exp Neurol 58:**313-320, 1999

132. Karino T, Goldsmith HL. Particle flow behavior in models of branching vessels. II. Effects of branching angle and diameter ratio on flow patterns. **Biorheology 22:**87-104, 1985

133. Pinchak AC, Ostrach S. Blood flow in branching vessels. **J Appl Physiol 41:**646-658, 1976

134. Ku DN, Giddens DP, Zarins CK, Glagov S. Pulsatile flow and atherosclerosis in the human carotid bifurcation. Positive cor-relation between plaque location and low oscillating shear stress. **Arteriosclerosis 5:**293-302, 1985

135. Schulz UG, Rothwell PM. Sex differences in carotid bifurcation anatomy and the distribution of atherosclerotic plaque. **Stroke 32:**1525-1531, 2001

136. Ruan L, Chen W, Srinivasan SR, Sun M, Wang H, Toprak A, et al. Correlates of common carotid artery lumen diameter in black and white younger adults: the Bogalusa Heart Study. **Stroke 40:**702-707, 2009

137. Lischka M, Krammer E, Rath T, Riedl M, Ellböck E. The human thyrocervical trunk: configuration and variability reinvestigated. **Anat Embryol (Berl) 163:**389-401, 1982

138. Thomas JB, Antiga L, Che SL, Milner JS, Steinman DA, Spence JD, et al. Variation in the carotid bifurcation geometry of young versus older adults: implications for geometric risk of atherosclerosis. **Stroke 36:**2450-2456, 2005

139. Gutierrez J, Rosoklija G, Murray J, Chon C, Elkind MS, Goldman J, et al. A quantitative perspective to the study of brain arterial remodeling of donors with and without HIV in the Brain Arterial Remodeling Study (BARS). **Front Physiol 5:**56, 2014

140. Gutierrez J, Goldman J, Honig LS, Elkind MSV, Morgello S, Marshall RS. Determinants of cerebrovascular remodeling: Do large brain arteries accommodate stenosis? **Atherosclerosis 235:**371-379, 2014

141. Chimowitz MI, Lynn MJ, Derdeyn CP, Turan TN, Fiorella D, Lane BF, et al. Stenting versus aggressive medical therapy for intracranial arterial stenosis. **N Engl J Med 365:**993-1003, 2011

142. Oates JW, McAuliffe W, Coates HL. Management of pseudo-aneurysm of a lateral aberrant internal carotid artery. **Int J Pediatr Otorhinolaryngol 42:**73-79, 1997

143. Uchino A. Bilateral persistent trigeminal artery variants diag¬nosed by MR angiography. **Cerebellum 10:**745-747, 2011

144. Siqueira M, Piske R, Ono M, Marino Júnior R. Cerebellar arteries originating from the internal carotid artery. **AJNR Am J Neuroradiol 14:**1229-1235, 1993

145. Celebi I, Oz A, Yildirim H, Bankeroglu H, Basak M. A case of an aberrant internal carotid artery with a persistent stapedial artery: association of hypoplasia of the A1 segment of the an¬terior cerebral artery. **Surg Radiol Anat 34:**665-670, 2012

146. Given CA 2nd, Huang-Hellinger F, Baker MD, Chepuri NB, Morris PP. Congenital absence of the internal carotid artery: case reports and review of the collateral circulation. **AJNR Am J Neuroradiol 22:**1953-1959, 2001

147. Luh GY, Dean BL, Tomsick TA, Wallace RC. The persistent fetal carotid-vertebrobasilar anastomoses. **AJR Am J Roentgenol 172:**1427-1432, 1999

148. Lasjaunias P, Théron J, Moret J. The occipital artery. Anatomy, normal arteriographic aspects, embryological significance. **Neuroradiology 15:**31-37, 1978

149. Guerri-Guttenberg RA. Fetal carotid-vertebrobasilar anastomoses: persistent hypoglossal artery associated with further variations of the circle of Willis. **Surg Radiol Anat 31:**311-315, 2009

150. Preul M, Tampieri D, Leblanc R. Giant aneurysm of the distal anterior cerebral artery: associated with an anterior communicating artery aneurysm and a dural arteriovenous fistula. **Surg Neurol 38:**347-352, 1992

151. Niizuma H, Kwak R, Uchida K, Suzuki J. Aneurysms of the azygos anterior cerebral artery. **Surg Neurol 15:**225-228, 1981

152. Parkinson D, Reddy V, Ross RT. Congenital anastomosis between the vertebral artery and internal carotid artery in the neck. Case report. **J Neurosurg 51:**697-699, 1979

153. Campos J, Fox AJ, Viñuela F, Lylyk P, Ferguson GG, Drake CG, et al. Saccular aneurysms in basilar artery fenestration. **AJNR Am J Neuroradiol 8:**233-236, 1987

154. Fujimura M, Sugawara T, Higuchi H, Oku T, Seki H. A ruptured aneurysm at the distal end of the basilar artery fenestration associated with multiple fenestrations of the vertebrobasilar system: case report. **Surg Neurol 47:**469-472, 1997

155. Scherer A, Siebler M, Aulich A. Virtual arterial endoscopy as a diagnostic aid in a patient with basilar artery fenestration and thromboembolic pontine infarct. **AJNR Am J Neuroradiol 23:**1237-1239, 2002

156. Anderson RA, Sondheimer FK. Rare carotid-vertebrobasilar anastomoses with notes on the differentiation between proatlantal and hypoglossal arteries. **Neuroradiology 11:**113-118, 1976

157. Oelerich M, Schuierer G. Primitive hypoglossal artery: demonstration with digital subtraction-, MR- and CT-angiography. **Eur Radiol 7:**1492-1494, 1997

158. Hacein-Bey L, Daniels DL, Ulmer JL, Mark LP, Smith MM, Strottmann JM, et al. The ascending pharyngeal artery: branches, anastomoses, and clinical significance. **AJNR Am J Neuroradiol 23:**1246-1256, 2002

159. Murai Y, Ikeda Y, Sato H, Yamamoto Y, Teramoto A. Anomalous internal carotid anastomosis to contralateral anterior cerebral artery. **Can J Neurol Sci 32:**359-360, 2005

160. LeMay M, Gooding CA. The clinical significance of the azy¬gos anterior cerebral artery (A.C.A.). **Am J Roentgenol Radium Ther Nucl Med 98:**602-610, 1966

161. Perlmutter D, Rhoton AL Jr. Microsurgical anatomy of the anterior cerebral-anterior communicating-recurrent artery complex. **J Neurosurg 45:**259-272, 1976

162. Alpers BJ, Berry RG. Circle of Willis in cerebral vascular disorders. The anatomical structure. **Arch Neurol 8:**398-402, 1963

163. Stock KW, Wetzel S, Kirsch E, Bongartz G, Steinbrich W, Radue EW. Anatomic evaluation of the circle of Willis: MR angiography versus intraarterial digital subtraction angiography. **AJNR Am J Neuroradiol 17:**1495-1499, 1996

164. Lasjaunias P, Santoyo-Vazquez A. Segmental agenesis of the internal carotid artery: angiographic aspects with embryological discussion. **Anat Clin 6:**133-141, 1984

165. Dimmick SJ, Faulder KC. Normal variants of the cerebral circulation at multidetector CT angiography. **Radiographics 29:**1027-1043, 2009

166. Rhoton AL Jr, Saeki N, Perlmutter D, Zeal A. Microsurgical anatomy of common aneurysm sites. **Clin Neurosurg 26:**248-306, 1979

167. Vasović L, Milenković Z, Pavlović S. Comparative morphological variations and abnormalities of circles of Willis: a mini review including two personal cases. **Neurosurg Rev 25:** 247-251, 2002

Ich möchte mich ganz herzlich bei Herrn PD Dr. Beseoglu für die stetige Mithilfe bei der Verfassung dieser Arbeit sowie für die dreijährige gemeinsame Arbeit am Universitätsklinikum in Düsseldorf bedanken. In dieser Zeit konnte ich nicht nur als Arzt, sondern auch als Mensch viel von ihm lernen.

Das größte Glück für einen Chirurgen besteht darin, einen großen Maestro als Vorbild zu haben. Dies ist für mich Herr Prof. Dr. Hans-Jakob Steiger, dem ich meine chirurgischen Fähigkeiten verdanke. Ich hoffe, dass ich weiterhin viel von ihm lernen darf, um ein guter Neurochirurg in und außerhalb des Operationssaals zu werden.

Zuletzt möchte ich mich ganz herzlich bei Herrn PD Dr. Cornelius sowie allen anderen Kolleginnen und Kollegen des Universitätsklinikums Düsseldorf, die mich auf meinem bisherigen Weg als Assistenzarzt in jeglicher Hinsicht inspiriert, gelehrt und unterstützt haben, bedanken.